

How Much do Heavy Quarks Thermalize in a Heavy Ion Collision?

Guy D. Moore

*Department of Physics, McGill University,
3600 rue University, Montréal QC H3A 2T8, Canada*

Derek Teaney

*Department of Physics & Astronomy,
SUNY at Stony Brook, Stony Brook, NY 11764, USA*

(Dated: February 2, 2008)

Abstract

We investigate the thermalization of charm quarks in high energy heavy ion collisions. To this end, we calculate the diffusion coefficient in the perturbative Quark Gluon Plasma and relate it to collisional energy loss and momentum broadening. We then use these transport properties to formulate a Langevin model for the evolution of the heavy quark spectrum in the hot medium. The model is strictly valid in the non-relativistic limit and for all velocities $\gamma v < \alpha_s^{-1/2}$ to leading logarithm in T/m_D . The corresponding Fokker-Planck equation can be solved analytically for a Bjorken expansion and the solution gives a simple estimate for the medium modifications of the heavy quark spectrum as a function of the diffusion coefficient. Finally we solve the Langevin equations numerically in a hydrodynamic simulation of the heavy ion reaction. The results of this simulation are the medium modifications of the charm spectrum R_{AA} and the expected elliptic flow $v_2(p_T)$ as a function of the diffusion coefficient.

I. INTRODUCTION

The experimental relativistic heavy ion program at RHIC aims to measure the properties of the Quark Gluon Plasma (QGP) [1]. One of the most exciting results from RHIC so far is the large azimuthal anisotropy of light hadrons with respect to the reaction plane, known as elliptic flow. Elliptic flow has been measured as a function of impact parameter, transverse momentum, rapidity and particle type and is quantified with $v_2(p_T)$ [2, 3, 4, 5, 6],

$$v_2(p_T) = \frac{\int d\phi \frac{dN}{p_T dp_T d\phi} \cos(2\phi)}{\int d\phi \frac{dN}{p_T dp_T d\phi}}. \quad (1.1)$$

The observed elliptic flow is significantly larger than was originally expected from kinetic calculations of quarks and gluons [7], but in fairly good agreement with simulations based upon ideal hydrodynamics [8, 9, 10, 11]. This result suggests that the medium responds as a thermalized fluid and that the transport mean free path is small [7, 12, 13].

However, this interpretation of the elliptic flow results is not universally accepted [14, 15]. Hadronization may amplify the underlying partonic elliptic flow [16]. Indeed, parton coalescence is one mechanism which may amplify the hadronic elliptic flow relative to its partonic constituents [15, 17, 18, 19, 20]. On physical grounds, it seems unlikely that the typical mean free path is much smaller than a thermal wavelength, $1/(2\pi T)$. Indeed it has recently been conjectured that the hydrodynamic diffusion coefficient $\eta/(e+p)$ is strictly larger than half a thermal wavelength [21],

$$\frac{\eta}{e+p} > \frac{1}{4\pi T}.$$

Here η is shear viscosity, $(e+p)$ is the enthalpy, and the ratio is a fundamental length scale in the QGP. If $\eta/(e+p)$ is significantly larger than this conjectured bound hydrodynamics would not be a viable explanation for the observed flow at RHIC. In this work we will accept the hydrodynamic paradigm of the RHIC results and study the correlated consequences of this interpretation.

Heavy quarks are a good probe of the transport properties of the medium. Given an estimate of the light quark relaxation time $\sim \eta/(e+p)$, the heavy quark relaxation time is

$$\tau_R \sim \frac{M}{T} \frac{\eta}{e+p},$$

where M is the mass of the heavy quark and T is the temperature. Thus, with $M \approx 1.4$ GeV and $T \approx 250$ MeV, we expect that the charm equilibration time is approximately 6 times larger than the light quark equilibration time. Since this factor is relatively large, we further expect that the elliptic flow of charm quarks will be smaller than the flow of light hadrons.

In addition, the heavy quarks are produced with a power-law transverse momentum spectrum which deviates strongly from the thermal spectrum. The relaxation time will control the extent to which the initial power-law spectrum approaches the thermal spectrum. Similarly, the relaxation time will control the extent to which the charm quark will follow the underlying flow of the medium. If the charm quark completely follows the flow of the medium then thermal spectrum is actually quite close to the perturbative spectrum and

it may be difficult to distinguish these two cases [19, 22]. Medium modifications of the heavy quark spectrum R_{AA} flow will be studied experimentally this year and will provide an experimental estimate of this relaxation time [23, 24, 25, 26, 27].

Most recent studies of the medium modifications of the charm spectrum have computed the energy loss of a heavy quark by gluon bremsstrahlung [28, 29, 30, 31]. In weak coupling (which is the framework in which all calculations have been performed), bremsstrahlung is the dominant energy loss mechanism only if the heavy quark is ultra-relativistic, $\gamma v \gg 1/g$. (Similarly, for an electron traversing a hydrogen target, bremsstrahlung losses first exceed ionization losses when $\gamma v \simeq 700$ [32].) For much of the measured momentum range, the heavy quark is not ultra-relativistic, $\gamma v \lesssim 4$, and in this case it is far from clear that radiative energy loss dominates over collisional energy loss.

About two thirds of all heavy quarks are produced with $p \lesssim M$, and therefore radiative energy loss should be neglected when studying bulk thermalization. When $\gamma v \gtrsim 4$, calculations do suggest that radiation dominates the *average* energy loss rate [33, 34]. However, as has been repeatedly emphasized [35, 36], the *average* energy loss is insufficient to describe the medium modifications of the spectrum R_{AA} . Collisions have a different fluctuation spectrum than radiation and therefore might contribute more to the suppression factor than was at first anticipated [37]. Since we are primarily interested here in heavy quarks with typical momenta $\gamma v \sim 1$, we will concentrate exclusively on elastic collisions.

Considering these points, we will re-examine collisional energy loss of a heavy quark in the perturbative QGP. Our tools are Hard Thermal Loop (HTL) perturbation theory and a heavy quark expansion ($M \gg T$). The average energy loss rate was first computed by Braaten and Thoma [38] and we will independently verify their results. (Recently this calculation was extended to anisotropic plasmas by Romatschke and Strickland [39].) We will also compute the rates of longitudinal and transverse momentum broadening which are essential to a complete calculation of the modification factor R_{AA} . We will relate all of these rates to the diffusion coefficient which we will compute. (In principle the diffusion coefficient of a heavy quark could have been gleaned from the results of Braaten and Thoma [38] and Svetitsky [40].) In perturbation theory, we can compare the diffusion coefficient of the heavy quark to the hydrodynamic time scale $\eta/(e+p)$ which was calculated previously [41, 42, 43]. Many of the ambiguities of perturbation theory cancel in the ratio of transport coefficients and we therefore hope to be able to extrapolate smoothly into the non-perturbative domain. Following this ideology, we express all of our phenomenological results in terms of the diffusion coefficient which may ultimately be determined from lattice QCD calculations.

With these transport properties in hand, we adopt a Langevin model for the equilibration of heavy quarks in heavy ion collisions. The Langevin equations correctly describe the kinetics of a heavy particle in a thermal medium and therefore naturally interpolate between a hydrodynamic regime at small momentum and a kinetic regime at large momentum. The model is similar to old work by Svetitsky [40] and was later used without fluctuations to estimate R_{AA} [34]. The model is strictly valid for non-relativistic quarks and for all velocities to leading logarithm in T/m_D . The corresponding Fokker-Planck equation is solved analytically in Section V for a Bjorken expansion. The solution provides a simple estimate for the modification factor R_{AA} and further elucidates the dynamics of equilibration. Then we solve the Langevin equations numerically in a hydrodynamic simulation of the heavy ion reaction. The results of the simulation are the medium modification factor R_{AA} and the corresponding elliptic flow $v_2(p_T)$ as a function of the diffusion coefficient.

Very recently, two papers have adopted a similar Langevin approach to address charm equilibration [44, 45]. The first of these papers [44] estimated possible non-perturbative contributions to the drag coefficient which may arise from quasi-hadronic bound states in the QGP. The second of these papers [45] estimated radiative and collisional energy loss, and found that collisional loss is significant even for rather energetic charm quarks, $E \sim 5 - 10$ GeV.

In addition, classical Boltzmann simulations by Molnar [46] and subsequent simulations by Zhang *et al.* [47] have studied how $v_2(p_T)$ and studied how $v_2(p_T)$ and R_{AA} depend on the charm mean free path. As is discussed in Section V C, the results of Molnar's simulation are comparable to the Boltzmann-Langevin approach adopted here.

Throughout, we will denote 4-vectors with capital letters P, Q and use \mathbf{p}, \mathbf{q} for their 3-vector components, p^0, q^0 for their energy components, and p, q for $|\mathbf{p}|, |\mathbf{q}|$. Our metric convention is $[-, +, +, +]$.

II. NON-RELATIVISTIC HEAVY QUARKS IN A THERMAL MEDIUM

First consider thermal heavy quarks, $M \gg T$, with typical thermal momentum $p \sim \sqrt{MT}$ and velocity $v \sim \sqrt{T/M} \ll 1$. Since $p \gg T$ it takes many collisions to change the momentum substantially. Even for hard collisions with momentum transfer $q \sim T$, it takes $\sim M/T$ collisions to change the momentum by a factor of order one. Therefore it is a good approximation to model the interaction of the heavy quark with the medium as uncorrelated momentum kicks. The momentum of the heavy quark will evolve according to the macroscopic Langevin equations [48]

$$\frac{dp_i}{dt} = \xi_i(t) - \eta_D p_i, \quad \langle \xi_i(t) \xi_j(t') \rangle = \kappa \delta_{ij} \delta(t - t'). \quad (2.1)$$

Here η_D is a momentum drag coefficient and $\xi_i(t)$ delivers random momentum kicks which are uncorrelated in time. 3κ is the mean squared momentum transfer per unit time. The solution of this stochastic differential equation is

$$p_i(t) = \int_{-\infty}^t dt' e^{\eta_D(t-t')} \xi_i(t'), \quad (2.2)$$

where we have assumed that $t \gg \eta_D^{-1}$. The mean squared value of p is

$$3MT = \langle p^2 \rangle = \int^0 dt_1 dt_2 e^{\eta_D(t_1+t_2)} \langle \xi_i(t_1) \xi_i(t_2) \rangle = \frac{3\kappa}{2\eta_D}, \quad (2.3)$$

and therefore

$$\eta_D = \frac{\kappa}{2MT}. \quad (2.4)$$

Now the diffusion constant in space, D , can be found by starting a particle at $x = 0$ at $t = 0$ and finding the mean squared position at a later time,

$$\langle x_i(t) x_j(t) \rangle = 2Dt \delta_{ij} \quad \rightarrow \quad 6Dt = \langle x^2(t) \rangle. \quad (2.5)$$

Using the relation between position and momentum

$$x_i(t) = \int_0^t dt' \frac{p_i(t')}{M}, \quad (2.6)$$

we have

$$6Dt = \int_0^t dt_1 \int_0^{t_1} dt_2 \frac{1}{M^2} \langle p(t_1)p(t_2) \rangle = \frac{6Tt}{M\eta_D}, \quad (2.7)$$

and therefore the diffusion constant is [48]

$$D = \frac{T}{M\eta_D} = \frac{2T^2}{\kappa}. \quad (2.8)$$

In the next paragraphs we will determine the mean squared momentum transfer per unit time, 3κ , and then the diffusion coefficient.

The only $2 \leftrightarrow 2$ scattering processes are $qH \rightarrow qH$ (H the heavy quark) and $gH \rightarrow gH$. The $qH \rightarrow qH$ process only occurs by t channel gluon exchange. Since in the rest frame of the plasma the Compton amplitude is suppressed by $v^2 \sim T/M$ (see Appendix B), the $gH \rightarrow gH$ process is also dominated by t channel gluon exchange. Kinematics demand that the transfer momentum be spatial up to $O(v)$ corrections, so the Hard Thermal Loop correction on the transferred gluon is described simply by Debye screening. Writing the incoming and outgoing momenta of the thermal particle as \mathbf{k} and \mathbf{k}' , and taking that particle's dispersion relation to be ultra-relativistic, the scattering matrix elements squared, summed on the colors and spins of the incoming thermal particles and over all quantum numbers of the final state particles, are (see Appendix B),

$$\begin{aligned} |\mathcal{M}|_{\text{quark}}^2 &= \left[2 \frac{C_H g^4}{2} \right] 16M^2 k_0^2 (1 + \cos \theta_{\mathbf{k}\mathbf{k}'}) \frac{1}{(q^2 + m_D^2)^2}, \\ |\mathcal{M}|_{\text{gluon}}^2 &= [N_c C_H g^4] 16M^2 k_0^2 (1 + \cos^2 \theta_{\mathbf{k}\mathbf{k}'}) \frac{1}{(q^2 + m_D^2)^2}. \end{aligned} \quad (2.9)$$

$C_H = C_F$ denotes the color Casimir of the heavy quark and an extra factor of 2 for the quark case accounts for anti-quarks.

The mean squared momentum transfer per unit time is 3κ . To compute this quantity the matrix elements must be integrated over the incoming momentum \mathbf{k} and outgoing momenta \mathbf{k}' , \mathbf{p}' , weighted by the appropriate statistical functions and by the squared momentum transfer $q^2 \equiv (\mathbf{k} - \mathbf{k}')^2$. The mean squared momentum transfer per unit time (3κ) is then

$$\begin{aligned} 3\kappa &= \frac{1}{2M} \int \frac{d^3\mathbf{k} d^3\mathbf{k}' d^3\mathbf{p}'}{(2\pi)^9 8k^0 k'^0 M} (2\pi)^3 \delta^3(\mathbf{p} + \mathbf{k}' - \mathbf{p}' - \mathbf{k}) 2\pi \delta(k' - k) \mathbf{q}^2 \times \\ &\quad \times [N_f |\mathcal{M}|_{\text{quark}}^2 n_f(k)(1 - n_f(k')) + |\mathcal{M}|_{\text{gluon}}^2 n_b(k)(1 + n_b(k'))]. \end{aligned} \quad (2.10)$$

In writing this formula we have used the non-relativistic limit $p^0 = p'^0 = M$. It is convenient to shift the \mathbf{p}' integration to an integral over the momentum transfer $\mathbf{q} \equiv \mathbf{p}' - \mathbf{p}$; the momentum conserving delta function becomes $\delta^3(\mathbf{k}' - \mathbf{q} - \mathbf{k})$. The appendix shows how a simple change of variables and an expansion in $m_D^2 \ll T^2$ makes these integrals relatively straightforward. Using the relation between κ and the diffusion coefficient Eq. (2.8), we find

$$D = \frac{36\pi}{C_H g^4 T} \left[N_c \left(\ln \frac{2T}{m_D} + \frac{1}{2} - \gamma_E + \frac{\zeta'(2)}{\zeta(2)} \right) + \frac{N_f}{2} \left(\ln \frac{4T}{m_D} + \frac{1}{2} - \gamma_E + \frac{\zeta'(2)}{\zeta(2)} \right) \right]^{-1}. \quad (2.11)$$

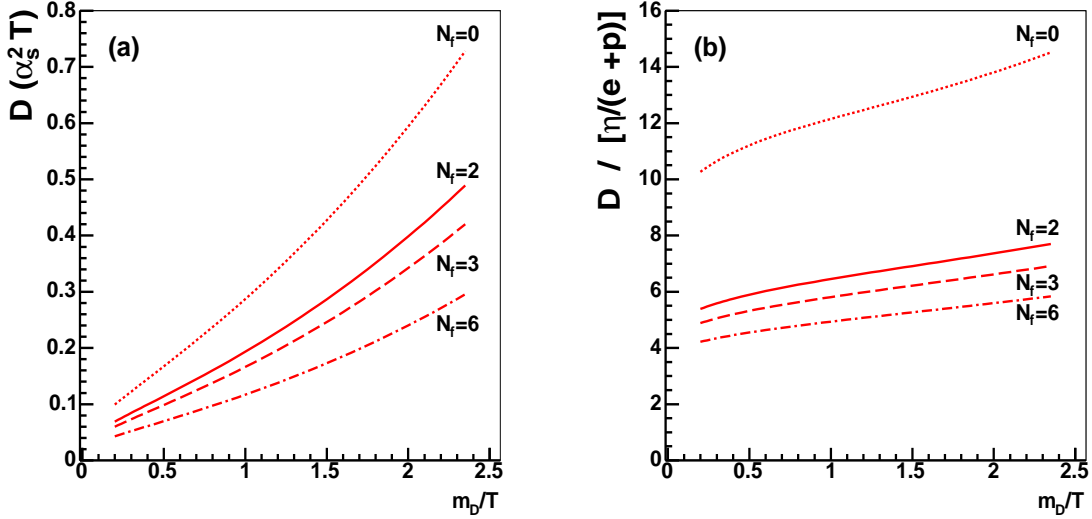


FIG. 1: (Color online) (a) The diffusion coefficient of a heavy quark in a QGP with N_f flavors of light quarks. (b) The ratio of the diffusion coefficient of a heavy quark to the hydrodynamic diffusion coefficient $\eta/(e+p)$.

This formula for the diffusion coefficient could have been extracted by combining the calculations of Braaten and Thoma [38] and Svetitsky [40]. Corrections to this expression are suppressed by at least one power of $\sqrt{\alpha_s}$; we expect corrections at that level.

This expression for the diffusion coefficient is based on a small m_D expansion and therefore becomes unreliable when the Debye mass becomes large. Rather than using a small m_D expansion we can numerically integrate Eq. (2.10) to determine the the diffusion coefficient. Something of this sort is necessary to deal with large values of m_D , but we emphasize that, at large values of m_D , the procedure is ad-hoc and should be considered only a qualitative guide. The m_D expansion would be a good approximation if the coupling were truly small. The numerical evaluation of the diffusion coefficient is illustrated in Fig. 1(a) as a function of m_D .

As discussed in the introduction, the time scale for equilibration $\tau \sim \frac{M}{T} \frac{\eta}{e+p}$. Now let us make this more concrete. The rate of equilibration is given by η_D^{-1} , as can be intuited from the Langevin equations, Eq. (2.1), or from the analysis of Section V. η_D^{-1} is directly related to the diffusion coefficient via

$$\frac{1}{\eta_D} = \frac{M}{T} D. \quad (2.12)$$

Taking $\alpha_s \approx 0.5$, $m_D/T \approx 1.5$, and $M/T \approx 7$ we estimate that the diffusion coefficient is $D \approx \frac{1.0}{T} \approx \frac{6}{2\pi T}$. The relaxation time is then $\eta_D^{-1} \approx 6.7/T$.

It is useful to compare this timescale with other hydrodynamic relaxation times in the QGP. The damping rate of sound waves in the QGP is controlled by $\eta/(e+p)$ where η is

the shear viscosity and $e + p$ is the enthalpy. Dividing by this ratio we have

$$\frac{1}{\eta_D} = \frac{M}{T} \frac{\eta}{e + p} \times \left[\frac{D}{\eta/(e + p)} \right]. \quad (2.13)$$

The quantity in square brackets is an estimate of the ratio between the heavy quark and hydrodynamic relaxation times and is illustrated in Fig. 1(b) as a function of m_D/T . Here the shear viscosity at leading order has been taken from [43]. As seen from the figure, for $N_f \approx 3$ the diffusion coefficient is ≈ 6 times larger than hydrodynamic scale $\eta/(e + p)$.

Both the calculation of the diffusion coefficient D and of the shear viscosity η are plagued by ambiguities when the coupling is strong, $\alpha_s > 0.2$. In particular, in both processes it is unclear how to screen the plasma when m_D is large and how to estimate the form and size of subleading α_s corrections. These issues have been discussed in [43], but were not resolved. However, since both processes are dominated by t -channel gluon exchange, the ambiguities in the calculation should largely cancel in the ratio of transport coefficients. We therefore hope that the computed factor of ≈ 6 for $D/[\eta/(e + p)]$ is largely independent of its perturbative assumptions. Thus, with $\frac{M}{T} \approx 7$, $T \approx 200$ MeV and an optimistic estimate of the shear viscosity, $\frac{\eta}{e+p} = 1/(6T)$, we estimate that the charm quark thermalization time is of order ≈ 7 fm. This time scale should be compared with the time scale for the development of elliptic flow ≈ 4 fm.

III. ENERGY LOSS

Since the initial distribution of charm quarks is much “harder” than a thermalized spectrum, it is important to study how higher energy heavy quarks, with $\gamma v \sim 1$, lose their energy in the thermal medium. We now turn to a discussion of this problem. Our discussion differs from most recent literature in that we take the dominant energy loss mechanism to be elastic scattering.

A. Why $2 \leftrightarrow 2$ dominates for $\gamma v \sim 1$

When the coupling is small, bremsstrahlung dominates the energy loss rate for very fast particles (with $\gamma v \sim 1/g$) while collisions dominate the rate for moderately relativistic particles with $\gamma v \sim 1$.

To see why, consider a heavy particle of momentum v , undergoing a scattering. Call its momentum P , with $p \equiv |\mathbf{p}| = vp^0$. For energy loss in a condensed medium, the scattering is typically off a nucleus, so the transferred 4-momentum Q^μ is purely spatial. In a thermal medium like the QGP, the scattering is off a relativistic particle at a random angle with respect to the heavy particle; the kinematics of the other particle requires that Q^μ be spacelike, but q^0 can be $\sim q \equiv |\mathbf{q}|$. Kinematics requires that the lightlike, bremmed particle’s momentum K satisfy $(K + P') = (Q + P)$, with P' the final particle momentum. K can be the largest if it is perfectly collinear with P and if Q is anti-collinear; in this case, energy conservation reads $k^0 = p^0 - p'^0 + q^0 = v(p - p') + q^0$, while momentum conservation reads $k = k^0 = p - p' - q$. For the spatial (Coulomb) scattering case, $k \leq vq/(1-v)$, while for the QGP case, $k \leq (vq+q^0)/(1-v)$, so the actual energy loss is $p^0 - p'^0 \leq v(q+q^0)/(1-v)$. In

either case, for $\gamma v \sim 1$, the energy of a bremsstrahlunged particle is at best of order of the transfer momentum in the scattering.

The energy loss in a scattering process without bremsstrahlung is q^0 . When $q^0 \sim T$ the plasma temperature, phase space favors events with q^0 negative and of order q . Since the rate of bremsstrahlung is suppressed by an additional factor of α_s , and the typical energy loss is the same, the contribution of bremsstrahlung to energy loss is smaller by a factor of α_s . In the soft region, $q \sim gT$, there is an approximate cancellation between energy losing and energy gaining scatterings, and the dominance of $2 \leftrightarrow 2$ processes is only by $\sqrt{\alpha_s}$, but they remain dominant. Softer momentum transfers are screened by the plasma and do not play an important role in energy loss.

Very similar arguments apply for electromagnetic energy loss of a high energy particle in a medium, except that the scale gT is played by the atomic radius and the $2 \leftrightarrow 2$ processes do not have any cancellation between energy losing and gaining processes; for $\gamma v \sim 1$, bremsstrahlung energy losses are subdominant to ionization losses (due to elastic scattering with electrons, transferring more energy than the electron's binding energy) by $Z\alpha$.

As the particle's energy increases, the importance of bremsstrahlung also increases. While the bremsstrahlung cross-section remains suppressed by a power of α_s , the amount of energy which can be lost in a single event increases. As we will see, the rate of energy loss by $2 \leftrightarrow 2$ processes only increases logarithmically in γv . Bremsstrahlung energy losses typically rise almost linearly in γv , and so become dominant at $\gamma v \sim 1/Z\alpha$ for electromagnetic processes and at $\gamma v \sim 1/\sqrt{\alpha_s}$ for heavy quark energy loss in the QGP. Since only a small tail of heavy quarks have $\gamma v \gg 1$, we will only treat $2 \leftrightarrow 2$ processes in this work.

B. Relativistic heavy quarks; momentum loss and momentum diffusion

First consider a heavy quark in a static medium with $p \gg T$ and velocity $\gamma v \sim 1$. It takes $\sim p/T$ collisions to change the momentum of the heavy quark by a factor of order one. The time between hard collisions is $\sim 1/(g^4T)$ and thus the equilibration time scale a heavy quark is of order $\sim (p/T) 1/(g^4T)$.

Next consider how a heavy quark with momentum $p \gg T$ changes over a time interval Δt which is long compared to the timescale of medium correlations but short compared to the time scale of heavy quark thermalization,

$$\frac{1}{g^4T} \ll \Delta t \ll \frac{p}{T} \frac{1}{g^4T}. \quad (3.1)$$

For Δt large compared to $1/(g^4T)$ the number of collisions N is large $\sim (\Delta t)(g^4T)$. On the other hand the momentum of the heavy particle has scarcely changed since the total momentum transferred Δp is of order $\Delta p \sim T(\Delta t)(g^4T)$ which is small compared to p . This means that the probability distribution for a given momentum transfer from a single collision is approximately constant over this time period. The accumulated momentum transfer is a sum of N such collisions. The sum of a large number of momentum transfers drawn from an identical probability distribution is approximately Gaussian plus corrections which go as $1/N$. In the next Δt time interval the process repeats itself independently. Thus we can write down a macroscopic equation of motion for the the heavy quark moving in the z

direction,

$$\begin{aligned}\frac{d}{dt}\langle p \rangle &\equiv -\eta_D(p)p, \\ \frac{1}{2}\frac{d}{dt}\langle(\Delta p_T)^2\rangle &\equiv \kappa_T(p), \\ \frac{d}{dt}\langle(\Delta p_z)^2\rangle &\equiv \kappa_L(p).\end{aligned}$$

Here $\langle(\Delta p_T)^2\rangle = \langle p_T^2 \rangle$ is the variance of the momentum distribution transverse to the direction of the heavy quark, $\langle(\Delta p_z)^2\rangle = (p_z - \langle p_z \rangle)^2$ is the variance of the momentum distribution in the direction parallel to the direction of the quark, and the time derivatives are understood to act only on a time scale of order Δt . The factor of $\frac{1}{2}$ in the transverse fluctuations has been inserted because there are two perpendicular directions. The functions η_D , κ_T , and κ_L encode the average momentum loss and the transverse and longitudinal fluctuations.

Now we will compute these coefficients using kinetic theory. First we will compute the mean rate of momentum loss. This is most easily done by computing the energy loss rate, dp^0/dt , which is related to the momentum loss by $dp^0/dt = v dp/dt$. The energy loss rate is found by multiplying the scattering rate with transfer energy q^0 , schematically,

$$\frac{dp}{dt} = \frac{1}{v} \int_{k,q} |\mathcal{M}|^2 q^0 f[k](1 \pm f[k-q^0]). \quad (3.2)$$

The factor q^0 is not enough to render this IR convergent, but there are cancellations between $q^0 > 0$ and $q^0 < 0$ contributions. It is easiest to account for these by averaging in the integrand over the process with k incoming and k' outgoing, and the process with k' incoming, k outgoing, and opposite Q^μ . Because we take $p \gg k$ the kinematics and matrix element are the same, but the population functions differ, yielding

$$\frac{dp}{dt} = \frac{1}{2v} \int_{k,q} |\mathcal{M}|^2 q^0 \{ f[k](1 \pm f[k-q^0]) - f[k-q^0](1 \pm f[k]) \}. \quad (3.3)$$

The population function here is $(e^{k/T} - e^{(k-q^0)/T})f[k]f[k-q^0]$, which vanishes at small q^0 and makes the integral well behaved.

Similarly, to compute the rate of transverse momentum broadening, we weight the transition rate $|\mathcal{M}|^2$ with the square of the transverse momentum transfer

$$\frac{d}{dt}\langle(\Delta p_T)^2\rangle = \int_{k,q} |\mathcal{M}|^2 q_T^2 f[k](1 \pm f[k-q^0]). \quad (3.4)$$

Here the integral will be convergent and we do not need to symmetrize over forward and backward collisions. Finally the rate of longitudinal momentum broadening is

$$\frac{d}{dt}\langle(\Delta p_z)^2\rangle = \int_{k,q} |\mathcal{M}|^2 q_z^2 f[k](1 \pm f[k-q^0]). \quad (3.5)$$

Again this integral is convergent. Thus to compute the transport coefficients η_D , κ_T , κ_L we need to specify the matrix elements and perform (numerically) the phase space integrals.

The covariant expressions for the scattering matrix elements in Eq. (2.9) (still summed over spins and colors of the bath particle), in vacuum, are

$$\begin{aligned} |\mathcal{M}|_{\text{quark}}^2 &= \left[2 \frac{C_H g^4}{2} \right] 16 \left[2 \frac{(P \cdot K)^2}{Q^4} - \frac{M^2}{2Q^2} \right], \\ |\mathcal{M}|_{\text{gluon}}^2 &= [N_c C_H g^4] 16 \left[2 \frac{(P \cdot K)^2}{Q^4} - \frac{M^2}{Q^2} + \frac{M^4}{4(P \cdot K)^2} \right], \end{aligned} \quad (3.6)$$

where $C_H = C_F$ is the quadratic Casimir of the heavy quark, P is the heavy particle 4-momentum, K is the light particle 4-momentum, Q is the 4-momentum transfer, and we use $[-, +, +, +]$ metric convention. The inclusion of Hard Thermal Loops is only necessary at small Q^2 , where the leading $1/Q^4$ term dominates; the details appear in the appendix. This introduces the Debye mass into the problem and thus the results will generally depend on the ratio of m_D/T .

Analytic expressions for the transport coefficients can be derived to leading logarithm in T/m_D . Without the Hard Thermal Loop correction the phase space integrals are logarithmically divergent at small q^2 . The leading log transport coefficient is found by evaluating the contribution to the phase-space integrals from the logarithmically divergent region $m_D^2 \ll q^2 \ll T^2$. This integral will give a log of T/m_D times some function of v . Further details are given in the appendix. We find that, to leading logarithm, the transport coefficients are

$$\frac{dp}{dt} \simeq v \left(N_c + \frac{N_f}{2} \right) \frac{C_H g^4 T^2}{24\pi} \left(\frac{1}{v^2} - \frac{1-v^2}{2v^3} \ln \frac{1+v}{1-v} \right) \ln(T/m_D), \quad (3.7)$$

$$\kappa_T \simeq \left(N_c + \frac{N_f}{2} \right) \frac{C_H g^4 T^3}{12\pi} \left(\frac{3}{2} - \frac{1}{2v^2} + \frac{(1-v^2)^2}{4v^3} \ln \frac{1+v}{1-v} \right) \ln(T/m_D), \quad (3.8)$$

$$\kappa_L \simeq \frac{2T}{v} \frac{dp}{dt}. \quad (3.9)$$

We note that the relation $\kappa_L = \frac{2T}{v} \frac{dp}{dt}$ is what is expected of the Boltzmann-Langevin approach. Indeed, the conclusion of the next section is that the Boltzmann-Langevin approach is strictly valid only in a leading-log approximation or in the non-relativistic limit. For completeness, the constant under the logarithm in Eqs. (3.7)–(3.9) is calculated in the appendix.

As for the diffusion coefficient, these expressions are only valid when the Debye mass is very small compared to the temperature. To extrapolate to finite m_D/T we return to the original expressions and numerically perform the phase-space integrals to determine the transport coefficients. The phase space integrals can be reduced to three dimensional integrals as is detailed in the appendix. The resulting transport coefficients and their dependence on the heavy quark momentum are illustrated in Fig. 2 and are discussed below.

The momentum dependence of the drag coefficient for various values of m_D/T is shown in Fig. 2(a). As above, we emphasize that these results are strictly valid only when the Debye mass is small and therefore the different curves illustrate the uncertainty in the calculation. The drag coefficient $\eta_D(p)$ has units $(\text{time})^{-1}$ and sets the equilibration rate. Since the drag coefficient at zero momentum is related to the diffusion coefficient which has already been discussed, we have divided by the drag coefficient at zero momentum to isolate the momentum dependence. We see that the equilibration rate $\eta_D(p)$ does not

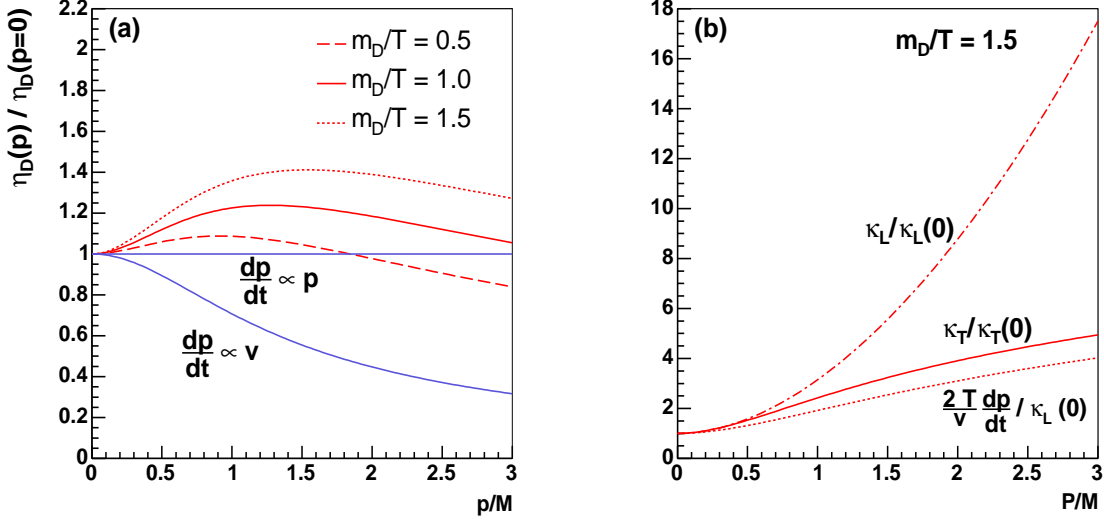


FIG. 2: (Color online) (a) The drag coefficient as a function of the heavy quark momentum, $\frac{dp}{dt} = \eta_D(p)p$. (b) The transverse ($\kappa_T(p)$) and longitudinal ($\kappa_L(p)$) momentum diffusion coefficients as a function of heavy quark momentum for $m_D/T = 1.5$. For comparison we also show the longitudinal momentum diffusion coefficient in a Boltzmann-Langevin approach ($\frac{2T}{v} \frac{dp}{dt}$).

decrease significantly with momentum. Only when the momentum is larger than $3M$ does the drag coefficient decrease. For comparison we have illustrated the expected form of the drag coefficient for an extreme model which is studied later. In this model, we have $\frac{dp}{dt} \propto v$ and therefore the equilibration time is inversely proportional to the energy of the heavy quark, $\eta_D \propto 1/E$.

Next we report on the transverse and longitudinal fluctuations for the heavy quark in Fig. 2(b). We see that both the transverse and longitudinal fluctuations ($\kappa_T(p)/\kappa_T(0)$ and $\kappa_L(p)/\kappa_L(0)$) rise with the momentum of the heavy quark. It is instructive to compare the longitudinal fluctuations derived from the full Boltzmann equation to the longitudinal fluctuations expected in a Boltzmann-Langevin approach described in the next section. In the Boltzmann-Langevin approach the longitudinal fluctuations are directly related to the drag through the relation

$$\frac{d}{dt} \langle (\Delta p_z)^2 \rangle = \frac{2T}{v} \frac{dp}{dt}.$$

We see that the Boltzmann-Langevin prediction for the longitudinal fluctuations ($\frac{2T}{v} \frac{dp}{dt}$) underestimates the fluctuations of the full Boltzmann equation (κ_L). At large momenta the underestimate can be a factor of 2 to 4.

IV. THE BOLTZMANN FOKKER-PLANCK EQUATION

The discussion in the previous sections (especially the first paragraph of Section III B) suggests a relativistic generalization of the non-relativistic Langevin equations. To this end,

we write a stochastic equation of motion for the heavy quark in the rest frame of the medium

$$\frac{dp_L}{dt} = -\eta_D(p)p^i + \xi_L, \quad (4.1)$$

$$\frac{dp_T}{dt} = \xi_T. \quad (4.2)$$

Here dp_L and dp_T are the momentum increments parallel and transverse to the direction of the heavy quark respectively. ξ_L and ξ_T are random momentum kicks in the longitudinal and transverse directions which satisfy

$$\langle \xi_L^i(t) \xi_L^j(t') \rangle = \kappa_L(p) \hat{p}^i \hat{p}^j \delta(t - t'), \quad (4.3)$$

$$\langle \xi_T^i(t) \xi_T^j(t') \rangle = \kappa_T(p) (\delta^{ij} - \hat{p}^i \hat{p}^j) \delta(t - t'), \quad (4.4)$$

$$\langle \xi_T^i(t) \xi_L^j(t') \rangle = 0. \quad (4.5)$$

Thus $\eta_D(p)p$ is the momentum loss per unit Δt and $\kappa_T(p)$ and $\kappa_L(p)$ are the variances of the transverse and longitudinal momentum transfers per unit Δt . From the discussion in Section III B, the precise momentum where $\eta_D(p)$ should be evaluated is known only up to corrections of order T/M .

The Langevin equation is ambiguous until it is discretized. If time is divided into discrete steps of Δt and the momenta at discrete times are labeled $\mathbf{p}^0, \mathbf{p}^1, \dots, \mathbf{p}^n$, then the Ito discretization of the Langevin equation is

$$(p^{n+1})^i - (p^n)^i = a_{\text{Ito}}^i(\mathbf{p}^n) \Delta t + \xi^i(\mathbf{p}^n) \Delta t,$$

where $\xi^i(\mathbf{p}^n)$ is drawn from the a Gaussian distribution such that

$$\langle \xi^i(\mathbf{p}^n) \xi^j(\mathbf{p}^m) \rangle = b^{ij}(\mathbf{p}^n) \frac{\delta^{mn}}{\Delta t},$$

and we have defined to coefficients $a^i(\mathbf{p})$ and $b^{ij}(\mathbf{p})$ as

$$a_{\text{Ito}}^i(\mathbf{p}) \equiv -\eta_D(p)p^i, \quad (4.6)$$

$$b^{ij}(\mathbf{p}) \equiv \kappa_L(p) \hat{p}^i \hat{p}^j + \kappa_T(p) (\delta^{ij} - \hat{p}^i \hat{p}^j). \quad (4.7)$$

With this choice of discretization, the Langevin equation is equivalent to a Fokker-Planck equation,

$$\frac{\partial P}{\partial t} + \frac{\partial}{\partial p^i} (a_{\text{Ito}}^i(\mathbf{p})P) - \frac{1}{2} \frac{\partial^2}{\partial p^i \partial p^j} (b^{ij}(\mathbf{p})P) = 0. \quad (4.8)$$

The most instructive way to show the equivalence between the Fokker-Planck and Langevin approach is to recognize that the Fokker-Planck equation is a Euclidean Schrödinger equation and therefore has a phase space path integral representation for the transition probability $P(\mathbf{p}, t | \mathbf{p}_0, t_0)$. (Here the canonical momenta and canonical coordinates are $\Pi = \frac{\partial}{\partial \mathbf{p}}$ and $Q = \mathbf{p}$, respectively.) Similarly it is easy to write down a path integral expression for the transition probability from the Langevin equations. The two path integrals are the same after integrating over canonical momenta [49].

Another equally valid discretization is the Stratonovich discretization of the Langevin equation

$$(p^{n+1})^i - (p^n)^i = a_{\text{Strat}}^i(\bar{\mathbf{p}}) \Delta t + \xi^i(\bar{\mathbf{p}}) \Delta t.$$

where $\bar{\mathbf{p}} = (\mathbf{p}^{n+1} + \mathbf{p}^n)/2$. This discretization will lead to a Fokker-Planck equation of the a slightly different form

$$\frac{\partial P}{\partial t} + \frac{\partial}{\partial p^i} (a_{\text{Strat}}^i(\mathbf{p})P) - \frac{1}{2} \frac{\partial}{\partial p^i} (b^{ij}(\mathbf{p}) \frac{\partial P}{\partial p^j}) = 0 .$$

Clearly the two forms of the Fokker-Planck equation will give the same answer if

$$a_{\text{Strat}}^i(p) = a_{\text{Ito}}^i(\mathbf{p}) - \frac{1}{2} \frac{\partial b^{ij}(\mathbf{p})}{\partial p_j} . \quad (4.9)$$

The resolution of this ambiguity was clarified by Arnold [49]. The correct procedure is to adjust the drag coefficient a^i so that the Fokker-Planck equation approaches equilibrium. We will discuss the Ito case here. Substituting the equilibrium distribution $P \propto e^{-E_p/T}$ into Eq. (4.8) and demanding that the r.h.s. return zero we obtain a relation between $a_{\text{Ito}}^i(\mathbf{p})$ and $b^{ij}(\mathbf{p})$. This relation, in terms of η_D , κ_L , and κ_T is

$$\begin{aligned} \eta_D^{(0)}(v) &\equiv \frac{\kappa_L(v)}{2TE} , \\ \eta_D^{\text{Ito}}(v) &= \eta_D^{(0)} - \frac{1}{E^2} \left[(1-v^2) \frac{\partial}{\partial v^2} (\kappa_L(v)) + \frac{d(\kappa_L(v) - \kappa_T v)}{v^2} \right] . \end{aligned} \quad (4.10)$$

Here $d = 3$ is the number of dimensions and v is the velocity of the heavy quark. The derivative term in square brackets is smaller by a factor of T/E than the first term and serves to renormalize the drag coefficient [49]. The derivative corrections to the drag coefficient a^i reflect the ambiguity in the momentum at which a^i is to be evaluated. Similarly, in the Stratonovich case we have $\eta_D^{\text{Strat}} \approx \eta_D^{(0)} + O(T/E)$. The $O(T/E)$ term can be deduced from the relation between the Stratonovich and Ito discretizations, Eq. (4.9).

In the previous section we computed in kinetic theory the drag coefficient to leading order in T/E , $\eta_D^{(0)}$. We also computed the longitudinal fluctuations κ_L to leading order in T/E . For the Fokker-Planck approach to be strictly valid the relation $\eta_D^{(0)}(p) = \kappa_L(p)/(2TE)$ must be satisfied; otherwise the stochastic process will not approach equilibrium. This is equivalent to the requirement that

$$\frac{d}{dt} \langle (\Delta p_z)^2 \rangle = \frac{2T}{v} \frac{dp}{dt} . \quad (4.11)$$

From kinetic theory we have the following equations for the drag and fluctuations:

$$\begin{aligned} \frac{dp}{dt} &= \frac{1}{2v} \int_{k,q} |\mathcal{M}|^2 q^0 \{ f[k](1 \pm f[k-q^0]) - f[k-q^0](1 \pm f[k]) \} , \\ \frac{d}{dt} \langle (\Delta p_z)^2 \rangle &= \int_{k,q} |\mathcal{M}|^2 q_z^2 \{ f[k](1 \pm f[k-q^0]) \} . \end{aligned}$$

In general, these two equations are not related to each other by the fluctuation dissipation relation, Eq. (4.11). However, if the transfer energy is small, $\omega \ll T$, we can expand the thermal distribution functions in the drag equation to the leading non-trivial order in ω to find

$$\begin{aligned} \frac{dp}{dt} &= \frac{1}{2vT} \int_{k,q} |\mathcal{M}|^2 \omega^2 \{ f[k](1 \pm f[k]) \} , \\ \frac{d}{dt} \langle (\Delta p_z)^2 \rangle &= \int_{k,q} |\mathcal{M}|^2 q_z^2 \{ f[k](1 \pm f[k]) \} . \end{aligned}$$

Upon using the simple kinematic formula $\omega = v q_z$ given in Appendix B, we find the required relation Eq. (4.11). Thus only when the transfer energy is small compared to the temperature is the Langevin model strictly valid.

The transfer energy is small only in two limiting cases. In the first case the heavy quark is non-relativistic. In this limit the energy transfer ω is less than the velocity times the momentum transfer, $\omega \leq v q$ and therefore is small compared to the temperature. If the quark is relativistic, however, ω is only small if the momentum transfer q is small compared to T . This is true only to leading-log of T/m_D . Thus we see that the leading-log transport coefficients (Eq. (3.7) and Eq. (3.9)) satisfy the fluctuation dissipation relation, Eq. (4.11).

This analysis indicates that an amalgamation of kinetic theory and the Langevin approach is correct to leading order. Given the two scales m_D and T , introduce q^* between m_D and T , say $q^* \sim \sqrt{m_D T}$. Then treat all collisions with large momentum transfer $q > q^* \gg m_D$ with ordinary unscreened kinetic theory. The kinetics of the hard collisions depends logarithmically on T/q^* . All collisions with momentum transfer $q < q^* \ll T$ can be subsumed into a Langevin process with prescribed transport coefficients that depend logarithmically on q^*/m_D . The dependence on q^* cancels when both the Langevin process and hard collisions are included. This procedure is only useful when m_D is really much smaller than T and we will not adopt it.

V. A LANGEVIN MODEL FOR HEAVY ION COLLISIONS

We have seen that, excepting non-relativistic quarks, the Langevin/Fokker-Planck approach is a valid description of the kinetics of heavy quarks only to leading logarithm in T/m_D . Since the coupling is not particularly small, this result says that the full kinetic theory should be used to find the evolution of the heavy quark spectrum.

However, the Langevin model is an appealingly simple framework for studying the thermalization of heavy quarks in a heavy ion collision. The Langevin model requires two inputs, the drag coefficient $\eta_D^{(0)}(v)$ and the transverse momentum fluctuations $\kappa_T(v)$. The longitudinal fluctuations are related to $\eta_D^{(0)}(v)$ by the fluctuation dissipation relation $\eta_D^{(0)}(v) = \kappa_L(v)/(2TE)$. (Finally the the drag coefficient can be tweaked as in Eq. (4.10) by terms suppressed by T/E so that the Langevin process approaches equilibrium.) As seen in Fig. 2(b), the longitudinal fluctuations in the Langevin model ($\frac{2T}{v} \frac{dp}{dt}$) are generally smaller than the corresponding fluctuations ($\kappa_L(p)$) in the full kinetic theory. The Langevin process will underestimate the longitudinal diffusion at high momentum by a factor of 2 to 4.

We have employed two models for the drag and transverse momentum diffusion coefficients. The first model is based on LO thermal QCD computation of the drag and transverse momentum diffusion coefficients. The procedure to set these coefficients is the following. First we set $m_D/T = 1.5$ and then use the results of Section III B to determine the momentum dependence of the coefficients, $\eta_D(p)/\eta_D(0)$ and $\kappa_T(p)/\kappa_T(0)$. Then $\eta_D(0)$ and $\kappa_T(0) = \kappa_L(0)$ are fixed by specifying the coefficient D and using the relation

$$\eta_D(0)^{-1} = \frac{M}{T} D = \frac{2TM}{\kappa_L(0)} .$$

This procedure is equivalent to simply adjusting α_s while leaving m_D/T fixed in the equations. This model is referred to as LO QCD below.

The second model is an extreme limit. In this case we set κ_L equal to a constant, which is equivalent to setting

$$\frac{dp}{dt} \propto v .$$

The transverse and longitudinal diffusion coefficients are then set equal to each other, $\kappa_T(v) = \kappa_L(v)$. The precise value of $\kappa_L(v)$ is specified by setting the diffusion coefficient as in the previous model.

We have also considered a third extreme limit. In this case we set $\eta_D(p)$ equal to a constant, which is equivalent to setting

$$\frac{dp}{dt} \propto p .$$

We have found that the results of this model are quite similar to the leading order model LO QCD as could have been intuited from Fig. 2(a). We will not discuss this model further.

A. Solution to the Fokker-Planck Equation for a Bjorken Expansion

Before considering this Langevin model for the drag and diffusion in detail, let us estimate the effects of thermalization on the spectrum of non-relativistic heavy quarks in a medium expanding in a boost invariant fashion. In this section we assume that the transport coefficients are evaluated at $v = 0$ where they are all related by constants, *i.e.* $\kappa = \kappa_L(0) = \kappa_T(0) = (2TM)\eta_D(0)$. In the non-relativistic limit the Langevin approach is strictly valid.

The Langevin update rule in the local rest frame is

$$\Delta \mathbf{x} = \frac{\mathbf{p}}{M} \Delta t , \tag{5.1}$$

$$\Delta \mathbf{p} = (-\eta_D \mathbf{p} + \xi) \Delta t , \tag{5.2}$$

where ξ is drawn from a Gaussian probability distribution of width $\langle \xi^i \xi^j \rangle = \kappa / \Delta t \delta^{ij}$. The Boltzmann-Fokker Planck Equation (BFPE) for this update rule is

$$\frac{\partial P}{\partial t} + \frac{p^i}{M} \frac{\partial P}{\partial x^i} = \left[\frac{\partial}{\partial p^i} \eta_D p^i + \frac{\partial^2}{\partial p^2} M T \eta_D \right] P(\mathbf{x}, \mathbf{p}, t) , \tag{5.3}$$

where $P(\mathbf{x}, \mathbf{p}, t)$ denotes the probability to observe a quark with position \mathbf{x} and momentum \mathbf{p} at time t . Our goal in the following paragraphs is to solve this partial differential equation for the evolution of the probability distribution for the simple case of a Bjorken expansion.

For a Bjorken expansion [50], the probability distribution is independent of the transverse coordinates and invariant under boosts in the z direction. This allows the BFPE to be simplified [51], and the Green function of the resulting partial differential equation is obtained in Appendix A. To obtain the final spectrum at time t we need to convolve this Green function $P(\mathbf{p}, t | \mathbf{p}_0, t_0)$ with the initial spectrum at time t_0 ,

$$\left. \frac{dN}{d^3p d\eta} \right|_{\eta=0,t} = \int d^3p_0 P(\mathbf{p}, t | \mathbf{p}_0, t_0) \left. \frac{dN}{d^3p_0 d\eta} \right|_{\eta=0,t_0} . \tag{5.4}$$

In this restricted sense of Eq. (5.4), $P(\mathbf{p}, t | \mathbf{p}_0, t_0)$ is the probability that the particle with momentum \mathbf{p}_0 at time t^0 evolves to a particle with momentum \mathbf{p} at some time t . $P(\mathbf{p}, t | \mathbf{p}_0, t_0)$ is given by

$$\begin{aligned} P(\mathbf{p}, t | \mathbf{p}_0, t_0) &= \frac{1}{\sqrt{2\pi M T^\perp(t)}} \exp \left[-\frac{(p_x - p_x^0 e^{-\chi(t)})^2}{2M T^\perp(t)} \right] \\ &\times \frac{1}{\sqrt{2\pi M T^\perp(t)}} \exp \left[-\frac{(p_y - p_y^0 e^{-\chi(t)})^2}{2M T^\perp(t)} \right] \\ &\times \frac{1}{\sqrt{2\pi M T^z(t)}} \exp \left[-\frac{(p_z - \left(\frac{t_0}{t}\right) p_z^0 e^{-\chi(t)})^2}{2M T^z(t)} \right], \end{aligned} \quad (5.5)$$

where we have defined the transverse and longitudinal effective temperatures,

$$\chi(t) = \int_{t_0}^t dt' \eta_D(t'), \quad (5.6)$$

$$T^\perp(t) = 2 \int_{t_0}^t dt' \eta_D(t') T(t') e^{2\chi(t') - 2\chi(t)}, \quad (5.7)$$

$$T^z(t) = 2 \int_{t_0}^t dt' \eta_D(t') T(t') \left(\frac{t'}{t}\right)^2 e^{2\chi(t') - 2\chi(t)}. \quad (5.8)$$

Now we will estimate how the initial spectrum of heavy charm quarks is changed by the interactions. For simplicity consider a Bjorken expansion with $T(t_0) = 300$ MeV, $t_0 = 1$ fm, $M = 1.4$ GeV. For an ideal Bjorken expansion, the temperature and drag coefficients follow [50]

$$T(t) = T(t_0) \left(\frac{t}{t_0}\right)^{-\frac{1}{3}}, \quad (5.9)$$

$$\eta_D(t) = \eta_D(t_0) \left(\frac{t}{t_0}\right)^{-\frac{2}{3}}. \quad (5.10)$$

$\eta_D(t_0)$ is adjusted according to Eq. (2.8) to give a specified diffusion coefficient. We will compute the spectrum of charm quarks at a final time $t_f = 6$ fm. The equilibrium temperature at this time is $T(t_f) = 165$ MeV. For the initial spectrum of heavy quarks we will take the transverse momentum spectrum from a fit to leading order parton model calculations which are described in the next section,

$$\frac{dN}{d\eta dy d^2 p_T} \propto \delta(y - \eta) \frac{1}{(p_T^2 + \Lambda^2)^\alpha}, \quad (5.11)$$

with $\alpha = 3.52$ and $\Lambda = 1.85$ GeV. The initial spectrum is shown in Fig. 3 and is labeled as LO pQCD. Then we convolve this initial condition with the Green function as in Eq. (5.4) to determine the final spectrum.

The final transverse momentum spectrum is shown as a function of the diffusion coefficient in Fig. 3. We observe that the charm spectrum approaches the thermal spectrum only when the diffusion coefficient is less than $3/(2\pi T)$. This is small relative to the estimates made

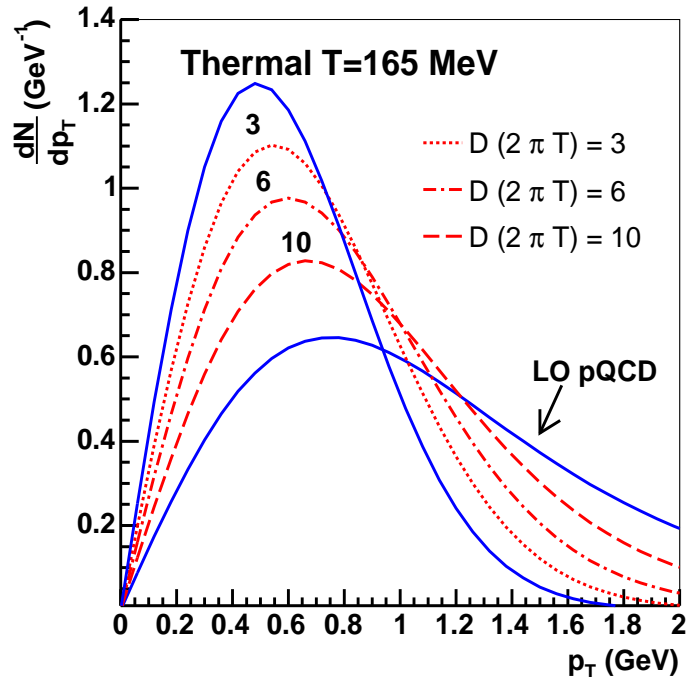


FIG. 3: (Color online) The transverse momentum spectrum of charm quarks at time $t_f = 6$ fm for a Bjorken expansion with $\tau_0 = 1$ fm and $T_0 = 300$ MeV and $T(t_f) = 165$ MeV. The initial transverse momentum spectrum is given by leading order perturbation theory (LO pQCD).

in the previous section. Further, such a small diffusion coefficient implies a substantial suppression of the spectrum at large transverse momentum. This basic observation will be quantitatively confirmed when we include radial flow in the next section. As studied in Appendix A, for large diffusion coefficients interactions simply smear the original spectrum (LO pQCD) with a Gaussian. For small diffusion coefficients the spectrum is close to the thermal spectrum ($T = 165$ MeV) up to small viscous corrections.

B. Elliptic Flow and Suppression of Charm Quarks

Next we will calculate how the flow of an underlying medium influences the spectrum of heavy quarks. If the relaxation time η_D^{-1} is less than the expansion rate of the medium, then the heavy quark will follow the medium. If η_D^{-1} is greater than the expansion rate, the heavy quark will not follow the medium and the resulting elliptic flow will be small. Of course, the relaxation time depends on the momentum of the heavy quark. The goal here is to determine the largest possible elliptic flow for a given value of the diffusion coefficient.

To this end we have placed heavy quarks into a hydrodynamic simulation of the heavy ion collision. In the local rest frame of the medium, the heavy quark follows the Langevin equations. Further discussion of Lorentz invariance and numerical implementation is given below.

The hydrodynamic simulation is a $2 + 1$ boost invariant hydrodynamic model with an ideal gas equation of state $p = \frac{1}{3}e$. The temperature is related to the energy density with

the $N_f = 3$ ideal QGP equation of state. We have chosen this extreme equation of state because the resulting radial and elliptic flow are too large relative to data on light hadron production. Thus, this equation of state will estimate the largest elliptic flow possible for a given diffusion coefficient.

Aside from the equation of state, the hydrodynamic model is based upon References [9]. At an initial time $\tau_0 = 1.0$ fm, the entropy is distributed in the transverse plane according to the distribution of wounded nucleons for a Au-Au collision with an impact parameter of $b = 6.5$ fm. Then one parameter $s_0 = 14 \text{ fm}^{-2}$, which is the entropy per unit rapidity per wounded nucleon per area, is adjusted to set the initial temperature and total particle yield. The value $s_0 = 14 \text{ fm}^{-2}$ closely corresponds to the results of full hydrodynamic simulations [9, 10, 11] and corresponds to a maximum initial temperature of $T_0 = 265$ MeV.

At the initial Bjorken time τ_0 , the position and momentum distributions of the heavy quarks are estimated from leading order parton model calculations. To this end, we have distributed the heavy quarks (about a million or so per run) in the transverse plane according to the distribution of binary collisions. In the longitudinal direction the heavy quarks are distributed uniformly in a large space-time rapidity window $\eta = -20 \dots 20$. Periodic boundary conditions are applied in the η direction. The initial momentum distribution is drawn from

$$\frac{dN}{dy d\eta d^2p_T} \propto \delta(y - \eta) \frac{1}{(p_T^2 + \Lambda^2)^\alpha}, \quad (5.12)$$

where $\alpha = 3.5$ and $\Lambda = 1.849$ GeV. This parameterization is a fit to leading order parton model calculations which were performed with the marvelous CompHEP package [52]. Specifically, charm production at mid-rapidity was computed for proton-proton collisions with $\sqrt{s} = 200$ GeV. The charm mass was set to 1.4 GeV and the strong coupling constant was evaluated at a scale $4m_T^2 = \hat{s} [1 - (-t + m_c^2/\hat{s})^2]$. Similarly the CETQ4m parton distributions were evaluated at a scale $4m_T^2$. The resulting momentum distribution is comparable to the results of Pythia calculations [53].

A few remarks about Lorentz invariance and numerical implementation are necessary. Consider a heavy quark with position and momentum 4-vectors $(x')^\mu$ and $(p')^\mu$ in a medium with four-velocity $u^\mu(x')$ in the computational frame. Given an infinitesimal time interval $\Delta t'$, we can calculate $\Delta \mathbf{x}'$ in the computational frame, *i.e.* $\Delta \mathbf{x}' = \frac{\mathbf{p}'}{E'} \Delta t'$. We therefore know the 4-vector $(\Delta x')^\mu$ and we can compute $(\Delta x)^\mu$ in the rest frame of the medium. In particular, we know the time interval in the rest frame Δt . In the rest frame, we can update the momentum using the Langevin rule. Now since the quark is on mass shell, the four momentum is known in the rest frame and can be boosted back to the computational frame. Generally there will be numerical artifacts which are not Lorentz invariant of order $\sqrt{\Delta t/L}$, where L is some typical time/length scale of change in the computational frame. Because of this dependence on Δt , it is important to check that Lorentz invariance is respected. Several test runs were performed in different frames to verify that numerical artifacts are under control at the 1.0% level when the γ factor u^0 is less than 15. The $\sqrt{\Delta t}$ error can presumably be avoided by employing a higher order algorithm for stochastic differential equations [54]. But, given the complexity of the intermediate boosts, the lowest order algorithm was adopted.

In summary, we place heavy quarks with a reasonable initial transverse momentum distribution in a hydrodynamic simulation of heavy ion collisions. Then the heavy quarks are

evolved according to the Langevin update rule in the local rest frame. We have simulated a solidly mid-central collision, $b = 6.5$ fm.

There are at least two items of experimental interest in the heavy ion program. The first is the suppression factor R_{AA} , which experimentally is the ratio of the proton-proton D meson spectrum to the Au-Au D meson spectrum. We will estimate R_{AA} at mid-rapidity using our “input” and “output” charm quark spectrum,

$$R_{AA} = \frac{\left(\frac{dN}{dp_T}\right)_{\text{output}}}{\left(\frac{dN}{dp_T}\right)_{\text{input}}}.$$

The “input” spectrum has already been described. Given the Langevin nature of the force, the spectrum never completely stops changing. However, the drag and fluctuations are proportional to powers of the temperature, and therefore their influence decreases at late times, as the temperature drops. We have found that the spectrum is nearly frozen after $\tau = 9$ fm. The “output” spectrum is really the spectrum at $\tau = 15$ fm. Integrating further would have only a negligible effect. A large unknown in the comparison to D meson data is how hadronization will affect the final spectrum. In the truly heavy quark limit, hadronization would not affect the spectrum significantly. However, the charm quark is not particularly heavy, and therefore various models of hadronization will give different answers. Coalescence and independent fragmentation are two extreme models which have been studied recently [19, 20]. We will ignore the important effects of hadronization in this work. Therefore, a direct comparison of our R_{AA} to the experimental R_{AA} is certainly misguided. The R_{AA} factor is illustrated in Fig. 4(a). This figure is discussed below.

A second item of experimental interest is elliptic flow. For simplicity we will consider only mid-rapidity. Elliptic flow is quantified with $v_2(p_T)$,

$$v_2(p_T) = \langle \cos(2\phi) \rangle_{p_T} = \frac{\int d\phi \frac{dN}{dy dp_T d\phi} \Big|_{y=0} \cos(2\phi)}{\int d\phi \frac{dN}{dy dp_T d\phi} \Big|_{y=0}}.$$

Here the angle ϕ is measured with respect to the reaction plane. The experimental determination of the reaction plane is discussed in [55, 56]. Again, we will estimate the elliptic flow of D mesons with our charm quark spectrum and ignore potential modifications due to hadronization. $v_2(p_T)$ is illustrated in Fig. 4(b).

To illustrate the model dependence, we have also calculated R_{AA} and $v_2(p_T)$ using two extreme models for the drag and fluctuations. As already elaborated, in the first model the drag is proportional to the velocity, $\frac{dp}{dt} \propto v$. The methods and caveats of extracting R_{AA} and $v_2(p_T)$ from the simulation are the same. The results are shown in Fig. 5(a) and (b). In the second model, the drag is proportional to the momentum, $\frac{dp}{dt} \propto p$. However, the results are not too different from the LO QCD model and therefore the results are not shown.

C. Comparison with Boltzmann Simulations

It is useful to compare our Boltzmann-Langevin approach to the classical Boltzmann simulations performed by Molnar [46] and subsequent simulations of Zhang *et al.* [47]. We

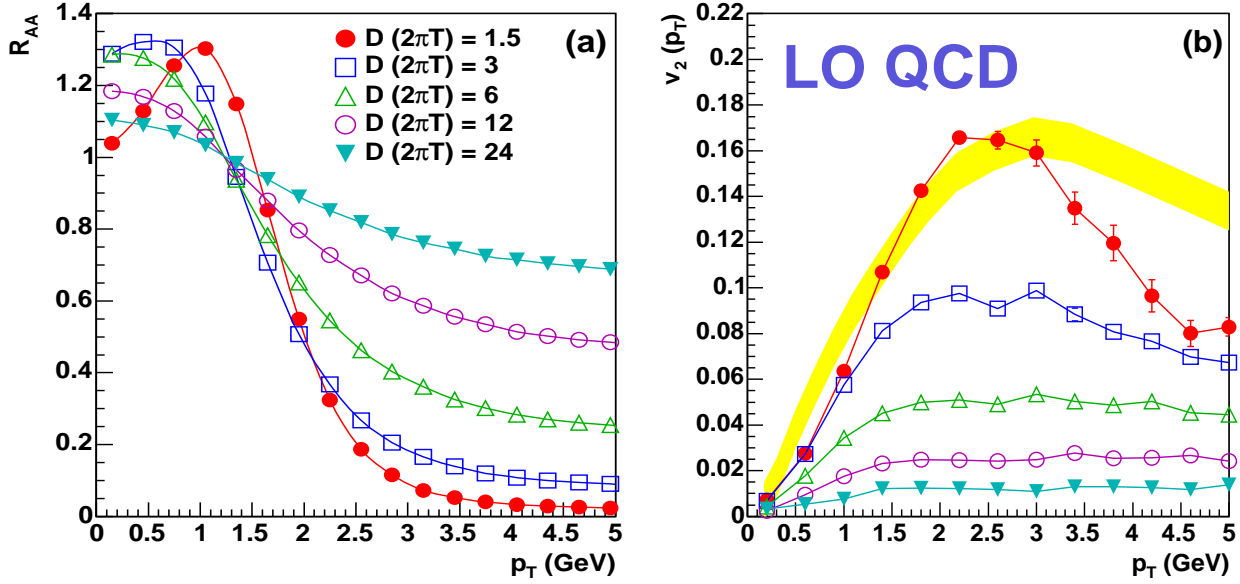


FIG. 4: (Color online) (a) The nuclear modification factor R_{AA} for charm quarks for representative values of the diffusion coefficient. (b) $v_2(p_T)$ for charm quarks for the same set of diffusion coefficients given in the legend in (a). In perturbation theory, $D \times (2\pi T) \approx 6 (0.5/\alpha_s)^2$. The model for the drag and fluctuation coefficients is referred to as LO QCD in the text. The band estimates the light hadron elliptic flow for impact parameter $b = 6.5$ fm using STAR data [2].

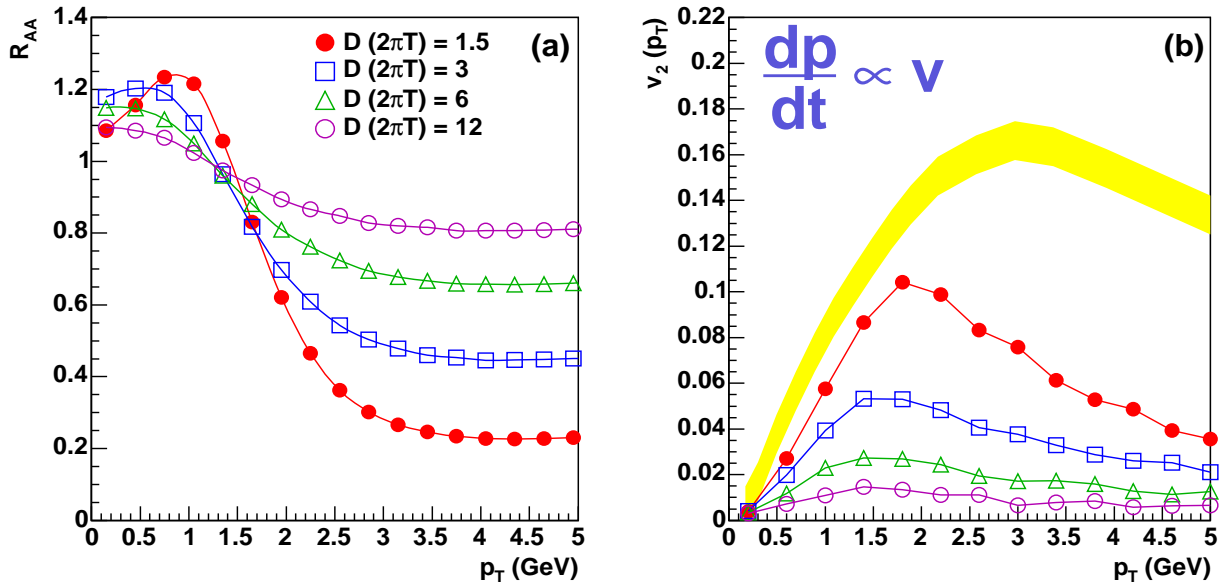


FIG. 5: (Color online) (a) The charm quark nuclear modification factor R_{AA} and (b) elliptic flow for representative values of the diffusion coefficient given in the legend. In this model, the drag is proportional to the velocity, $\frac{dp}{dt} \propto v$. For further explanation see Fig. 4.

will concentrate on Molnar's simulation here. In this simulation the gluon-gluon cross section takes the form, $\frac{d\sigma}{dt} \propto 1/(t - \mu_D^2)^2$, with screening mass, $\mu_D = 0.7 \text{ GeV}$. The total gluon-gluon cross section fixes α_s through the relation $\sigma_0 = \frac{9\pi\alpha_s^2}{2\mu_D^2}$. The constants are determined by comparing the model cross sections at finite t and zero μ_D with the corresponding unscreened perturbative expressions in QCD. The extracted α_s is used to set the charm-quark cross sections. To estimate the diffusion coefficient in this model we follow Appendix B 2, suitably modified for the classical statistics in Molnar's simulation. The diffusion coefficient of the charm quark in this model can be written in the follow form:

$$D = \frac{1}{(C_F/C_A) n_0 \sigma_0} f\left(\frac{\mu_D}{T}, \frac{n_q}{n_g}\right), \quad (5.13)$$

where n_g is the density of gluons, n_q is the density of quarks plus anti-quarks, $n_0 = n_g + n_q$ is the total particle density, and the function $f(\mu_D/T, n_q/n_g)$ is determined after Appendix B 2. $f(\mu_D/T, n_q/n_g)$ is approximately two for typical simulation parameters.

The magnitude of the resulting elliptic flow in Molnar's classical Boltzmann simulation, with $\frac{dN}{dy} = 2000$ for central collisions and $\sigma_0 = 10 \text{ mb}$, is similar to our results with $D \approx 3/(2\pi T)$. Since elliptic flow develops over a period of 1–4 fm we will estimate the diffusion coefficient at $\tau \approx 2 \text{ fm}$ in Molnar's simulation and compare it with $D \approx 3/(2\pi T)$. The precise value of Molnar's diffusion coefficient depends on μ_D/T , which we take to be 2.5. It also depends on the ratio of quarks to gluons which we take to be $n_q/n_g = 36/16$ for chemically equilibrated 3-flavor matter and $n_q/n_g = 0$ for gluon dominated matter. Using Glauber calculations, we estimate the transverse area for central collisions to be $A = 100 \text{ fm}^2$. Then, $n_0 = (dN/dy)/(\tau A)$. With these inputs, the diffusion coefficient in Molnar's model is

$$D|_{\tau \approx 2 \text{ fm}} \approx 0.225 \text{ fm} \begin{cases} 1.4 & \text{(gluon dominated)} \\ 2.5 & \text{(chemically equilibrated)} \end{cases}. \quad (5.14)$$

Taking $T \approx 200 \text{ MeV}$ and $D \approx 3/(2\pi T)$, the diffusion coefficient in our model is

$$D|_{\tau \approx 2 \text{ fm}} \approx 0.47 \text{ fm}. \quad (5.15)$$

Comparing Eq. (5.14) and Eq. (5.15) we conclude that both approaches agree on the magnitude of the elliptic flow when the transport coefficients are comparable. Our simulation with $D = 3/(2\pi T)$ corresponds to Molnar's simulation with $dN/dy = 2000$ for central collisions and $\sigma_0 = 10 \text{ mb}$.

VI. DISCUSSION

Fig. 4(a) and (b) summarize the phenomenological application of our work. Several items are apparent in these figures.

First, we see in Fig. 4(a) that there is no significant suppression in R_{AA} until the diffusion coefficient is of order, $D \approx 20/(2\pi T)$. This diffusion coefficient should be compared with the perturbative estimate made in Section II,

$$D \approx \frac{6}{2\pi T} \left(\frac{0.5}{\alpha_s}\right)^2. \quad (6.1)$$

The suppression seen in Fig. 4(a) at large transverse momentum, $p_T \gtrsim 4.0$ GeV, is somewhat overestimated since the Langevin description underestimates the longitudinal fluctuations by a factor of three to four in this momentum range. However, for $p_T \gtrsim 4.0$ GeV radiation should become important and further suppress the spectrum.

Examining Fig. 4(a) at large momentum, we see that the suppression decreases only slightly for p_T greater than ≈ 3 GeV. This is reminiscent of the suppression pattern seen in the light hadron data. It seems that all calculation which have a reasonably complete model of the fluctuations can reproduce this trend [36, 57]. This suppression pattern is approximately independent of the model for the transport coefficients. Looking at Fig. 5(a), we see essentially the same pattern when $\frac{dp}{dt} \propto v$. However, in this case the magnitude of the suppression is significantly smaller for a given value of the diffusion coefficient.

Turning to elliptic flow, we see in Fig. 4(b) that the heavy quark elliptic flow rises with momentum until $p_T \approx 1 - 2$ GeV, and then flattens. (When $D = 1.5/(2\pi T)$, $v_2(p_T)$ shows a qualitatively different behavior which will be discussed shortly.) A similar transition is seen in the elliptic flow of light hadrons, illustrated by the band in the figure. For the light hadron data, it has been argued that the transition from rising to flat is controlled by transport coefficients, and signals a transition from a quasi-thermal to a kinetic regime [7, 13]. A similar argument can be given here. Examining Fig. 4(a), we see that R_{AA} has a funny shape at low momentum and then starts to fall exponentially. These features reflect the thermal distribution. At higher momentum, R_{AA} stops falling exponentially and approaches a constant. This transition coincides with the transition seen in $v_2(p_T)$ and depends on the diffusion coefficient. A detailed study of the correlation between the initial angle of the charm quark and the final angle of the charm quark confirms the qualitative conclusion that the changes seen in v_2 and R_{AA} for $p_T \approx 1 - 2$ GeV reflect a transition from a quasi-thermal to a kinetic regime. Only models which smoothly interpolate between these two regimes can effortlessly reproduce these trends in the entire p_T range.

It has been argued that the charm quark could participate in the flow, and thus be pushed out to higher transverse momentum [19, 22]. This scenario depends on the diffusion coefficient. A detailed analysis of the initial and final momenta of the charm quarks shows that, unless the diffusion coefficient is $\approx 1.5/(2\pi T)$ or less, the charm quarks are not pushed to higher momentum by the flow. Indeed, when the diffusion coefficient is greater than $1.5/(2\pi T)$, a particle with final momentum 1.8 GeV typically started with momentum larger than this value. When the diffusion coefficient is small, $D \lesssim 1.5/(2\pi T)$, the heavy quarks are pushed out to higher momentum by the flow. This push is reflected in the p_T dependence of the elliptic flow, as illustrated in Fig. 4(b). The rapid fall of $v_2(p_T)$ for $p_T \approx 3.0$ GeV indicates that the hydrodynamics is not able to push the heavy quarks beyond this transverse momentum for this diffusion coefficient.

The p_T dependence of the elliptic flow also reflects aspects of the underlying QCD matrix elements. In contrast to a constant energy loss model, where $\frac{dp}{dt} \propto v$, the LO QCD drag coefficient rises with the momentum of the heavy quark (see Fig. 2(a)). Consequently, in the constant energy loss model, the elliptic flow decreases steadily at large momentum rather than remain constant as in the LO QCD model. The elliptic flows of the two models are compared in Fig. 4(b) and Fig. 5(b).

Examining Fig. 4(a) and (b), we reach the important conclusion that R_{AA} and $v_2(p_T)$ are tightly correlated. At low momentum, this correlation is encoded in Einstein's relation

between the energy loss and the hydrodynamic diffusion coefficient,

$$\left. \frac{dE}{dx} \right|_{v \approx 0} = \frac{T}{D}.$$

It is impossible to have a large elliptic flow without also predicting a significant suppression of charm quarks. Indeed, if future measurements find the charm elliptic flow strong, and the spectrum not suppressed, the present authors must logically conclude that hydrodynamics is not responsible for the observed elliptic flow. This strong conclusion might be mitigated if coalescence or some other exotic hadronization mechanism manages to make the D meson elliptic flow significantly larger than the underlying c -quark elliptic flow.

This point is underscored in recent classical Boltzmann simulations by Molnar [46] and subsequent simulations by Zhang *et al.* [47]. We found in Section VC that our charm quark elliptic flow is comparable to Molnar's results, provided the two simulations have approximately the same diffusion coefficient. Our simulation with $D = 3/(2\pi T)$ corresponds to his simulation with $dN/dy = 2000$ for central collisions and $\sigma_0 = 10$ mb. However, in Molnar's work, the final D-meson elliptic flow is significantly larger than the underlying c -quark flow as a result of coalescence. Similarly in the simulation of Zhang *et al.*, the final D-meson elliptic flow is amplified by coalescence, although the amplification factor is smaller than in Molnar's work due to the details of the coalescence model. Whether coalescence can amplify the elliptic flow of D-mesons in a complete dynamical setting remains unclear [57, 58].

In summary, we have calculated various transport coefficients for a heavy fermion in the perturbative Quark Gluon Plasma. Since the gamma factor of the charm quark is not particularly large in much of the experimental momentum range, $\gamma v \lesssim 4$, collisions rather than radiation should determine the medium modifications of the heavy quark spectrum. Therefore, we have re-examined collisional energy loss, and also calculated momentum broadening, which is essential to determine how the heavy quark spectrum will be modified. To quantitatively assess the modifications of the heavy quark spectrum, we formulated a Boltzmann-Langevin model for the heavy quark kinetics. The model is strictly valid for non-relativistic quarks and for relativistic quarks to leading log of T/m_D . We characterized the strength of the energy loss and momentum diffusion in terms of the diffusion coefficient, which in perturbation theory is approximately, $D \times (2\pi T) \approx 6 (0.5/\alpha_s)^2$. The Boltzmann-Langevin model was solved analytically for a Bjorken expansion, giving a simple estimate shown in Fig. 3 for the medium modifications of the heavy quark spectrum. Then we solved the Langevin equations numerically, yielding the modification factor R_{AA} and $v_2(p_T)$ for charm quarks. The results are shown in Fig. 4(a) and (b).

The diffusion coefficient for a relativistic plasma is of order $\sim \tau_c$, where τ_c is the typical collision time of the heavy quark. Thus, future measurements at RHIC will produce a tantalizing estimate of this fundamental time scale. Since the diffusion coefficient is a well defined concept, this estimate might ultimately be compared to Lattice QCD calculations, confirming or rejecting the paradigm of QGP formation in relativistic heavy ion collisions.

Acknowledgments. We thank Peter Petreczky for useful discussions. This work was supported by grants from the U.S. Department of Energy, DE-FG02-88ER40388 and DE-FG03-97ER4014, from the Natural Sciences and Engineering Research Council of Canada, and from le Fonds Québécois de la Recherche sur la Nature et les Technologies.

APPENDIX A: SOLUTION OF THE FOKKER-PLANK EQUATION FORK A BJORKEN EXPANSION

Our starting point is the Boltzmann-Fokker Planck Equation (BFPE) for the probability $P(\mathbf{x}, \mathbf{p}, t)$ to find a particle at (\mathbf{x}, \mathbf{p}) ,

$$\frac{\partial P}{\partial t} + \frac{p^i}{M} \frac{\partial P}{\partial x^i} = \left[\frac{\partial}{\partial p^i} \eta_D p^i + \frac{\partial^2}{\partial p^2} MT \eta_D \right] P(\mathbf{x}, \mathbf{p}, t). \quad (\text{A1})$$

It is important to remember that P depends on space and time through the flow velocity and temperature dependences of the medium.

For a Bjorken expansion, the probability distribution is independent of the transverse coordinates and invariant under boosts in the z direction. This allows the l.h.s. of the BFPE to be simplified [51]. Without loss of generality, we can restrict our attention to mid-rapidity, $z = 0$. Demanding that the probability distribution be invariant under small longitudinal boosts leads to the requirement that

$$t \frac{\partial P(z, p^\perp, p_z)}{\partial z} \Big|_{z=0} = -M \frac{\partial P(z, p^\perp, p_z)}{\partial p_z} \Big|_{z=0}, \quad (\text{A2})$$

where we have used the non-relativistic approximation $E = M$, and where p_a^\perp denotes the transverse vector, *i.e.* $p_a^\perp = (p_x, p_y)$. With the standard substitutions [51],

$$\bar{p}_z \equiv p_z \frac{t}{t_0}, \quad (\text{A3})$$

$$P(t, p_z) \equiv \bar{P}(t, \bar{p}_z), \quad (\text{A4})$$

and Eq. (A2), the BFPE reads,

$$\frac{\partial \bar{P}}{\partial t} = 3\eta_D \bar{P} + \eta_D p_a^\perp \frac{\partial \bar{P}}{\partial p_a^\perp} + \eta_D \bar{p}_z \frac{\partial \bar{P}}{\partial \bar{p}_z} + MT \eta_D \frac{\partial^2 \bar{P}}{\partial p_a^\perp \partial p_a^\perp} + MT \eta_D \left(\frac{t}{t_0} \right)^2 \frac{\partial^2 \bar{P}}{\partial \bar{p}_z^2}. \quad (\text{A5})$$

This may be turned into the diffusion equation by employing the method of characteristics [48]. With the following substitutions,

$$u_a^\perp(t) = p_a^\perp e^{\int_{t_0}^t dt \eta_D}, \quad (\text{A6})$$

$$u_z(t) = \bar{p}_z e^{\int_{t_0}^t dt \eta_D}, \quad (\text{A7})$$

$$\bar{P}(t, p_a^\perp, \bar{p}_z) = f(t, u^\perp, u_z) e^{3 \int_{t_0}^t dt \eta_D}, \quad (\text{A8})$$

Eq. (A5) becomes

$$\frac{\partial f}{\partial t} = MT \eta_D e^{2 \int_{t_0}^t dt \eta_D} \frac{\partial^2 f}{\partial u_a^\perp \partial u_a^\perp} + MT \eta_D \left(\frac{t}{t_0} \right)^2 e^{2 \int_{t_0}^t dt \eta_D} \frac{\partial^2 f}{\partial u_z^2}. \quad (\text{A9})$$

Employing separation of variables and one more change of variables, we write

$$f(t, u^\perp, u_z) = f_x(\theta^\perp, u_x) f_y(\theta^\perp, u_y) f_z(\theta_z, u_z), \quad (\text{A10})$$

with

$$\theta^\perp \equiv \int_{t_0}^t MT\eta_D e^{2\int_{t_0}^t dt \eta_D} , \quad (\text{A11})$$

$$\theta_z \equiv \int_{t_0}^t MT\eta_D \left(\frac{t}{t_0}\right)^2 e^{2\int_{t_0}^t dt \eta_D} , \quad (\text{A12})$$

and find three uncoupled diffusion equations,

$$\frac{\partial f_x}{\partial \theta^\perp} = \frac{\partial^2 f_x}{\partial u_x^2} , \quad (\text{A13})$$

$$\frac{\partial f_y}{\partial \theta^\perp} = \frac{\partial^2 f_y}{\partial u_y^2} , \quad (\text{A14})$$

$$\frac{\partial f_z}{\partial \theta_z} = \frac{\partial^2 f_z}{\partial u_z^2} . \quad (\text{A15})$$

The Green function for the diffusion equation is well known,

$$f_x(\theta^\perp, u_x) = \frac{1}{\sqrt{4\pi\theta^\perp}} e^{-\frac{u_x^2}{4\theta^\perp}} . \quad (\text{A16})$$

Unraveling the nested definitions, we find the following Green function for the BFPE for a Bjorken expansion:

$$\begin{aligned} P_z(\mathbf{p}, t|\mathbf{p}_0, t_0) &= \frac{1}{\sqrt{2\pi MT^\perp(t)}} \exp\left[-\frac{(p^x - p_0^x e^{-\chi(t)})^2}{2MT^\perp(t)}\right] \\ &\times \frac{1}{\sqrt{2\pi MT^\perp(t)}} \exp\left[-\frac{(p^y - p_0^y e^{-\chi(t)})^2}{2MT^\perp(t)}\right] \\ &\times \frac{t_0}{t} \frac{1}{\sqrt{2\pi MT^z(t)}} \exp\left[-\frac{(p^z - \left(\frac{t_0}{t}\right) p_0^z e^{-\chi(t)})^2}{2MT^z(t)}\right] , \end{aligned} \quad (\text{A17})$$

with the intuitive definitions:

$$\chi(t) = \int_{t_0}^t dt' \eta_D(t') , \quad (\text{A18})$$

$$T^\perp(t) = 2 \int_{t_0}^t dt' \eta_D(t') T(t') e^{2\chi(t') - 2\chi(t)} , \quad (\text{A19})$$

$$T^z(t) = 2 \int_{t_0}^t dt' \eta_D(t') T(t') \left(\frac{t'}{t}\right)^2 e^{2\chi(t') - 2\chi(t)} . \quad (\text{A20})$$

Switching from z to η coordinates, we define $P(\mathbf{p}, t|\mathbf{p}_0, t_0) \equiv (t/t_0)P_z(\mathbf{p}, t|\mathbf{p}_0, t_0)$ and have

$$\left. \frac{dN}{d^3p d\eta} \right|_{\eta=0,t} = \int d^3p_0 P(\mathbf{p}, t|\mathbf{p}_0, t_0) \left. \frac{dN}{d^3p_0 d\eta} \right|_{\eta=0,t_0} . \quad (\text{A21})$$

The differences between the transverse and longitudinal directions of the Green function should be noted.

Now let us substitute the form expected for the Bjorken solution into these equations. Noting that $\eta_D \propto T^2$, we have

$$T(t) = T(t_0) \left(\frac{t}{t_0} \right)^{-\alpha}, \quad (\text{A22})$$

$$\eta_D(t) = \eta_D(t_0) \left(\frac{t}{t_0} \right)^{-2\alpha}. \quad (\text{A23})$$

Defining $\chi_0 \equiv \eta_D(t_0) t_0 / (1 - 2\alpha)$ and changing integration variables to integrate over χ produces

$$\chi = \chi_0 \left[\left(\frac{t}{t_0} \right)^{1-2\alpha} - 1 \right], \quad (\text{A24})$$

$$T^\perp(t) = T(t) h_{\frac{-\alpha}{1-2\alpha}}(2\chi + 2\chi_0) - e^{-2\chi} T(t_0) h_{\frac{-\alpha}{1-2\alpha}}(2\chi_0), \quad (\text{A25})$$

$$T^z(t) = T(t) h_{\frac{2-\alpha}{1-2\alpha}}(2\chi + 2\chi_0) - e^{-2\chi} T(t_0) \left(\frac{t_0}{t} \right)^2 h_{\frac{2-\alpha}{1-2\alpha}}(2\chi_0). \quad (\text{A26})$$

Here we have defined the function

$$h_\gamma(x) = \begin{cases} x^{-\gamma} e^{-x} \int_0^x dx' x'^\gamma e^{x'} & \gamma > -1 \\ x e^{-x} \text{Ei}(x) & \gamma = -1 \end{cases},$$

and employed the exponential integral $\text{Ei}(z) = -\int_{-z}^\infty dt e^{-t}/t$. $h_\gamma(x)$ may be expressed in terms of the incomplete gamma function, but we did not find the results useful in developing the series expansions below. For small x we have

$$h_\gamma(x) \approx \begin{cases} \frac{x}{\gamma+1} - \frac{x^2}{(\gamma+1)(\gamma+2)} + \dots & \gamma > -1 \\ (\ln(x) + \gamma_E) x - (-\ln(x) - \gamma_E + 1) x^2 + \dots & \gamma = -1 \end{cases}, \quad (\text{A27})$$

where $\gamma_E \approx 0.5772$ is the Euler-Mascheroni constant. For large x and all values of γ we have

$$h_\gamma(x) \approx 1 - \frac{\gamma}{x} + \frac{\gamma(\gamma-1)}{x^2} + \dots + O(e^{-x}). \quad (\text{A28})$$

For small values of χ and χ_0 the heavy quark spectrum is only slightly affected by the surrounding medium. Using the small argument expansion of $h_\gamma(x)$, we have for small values of χ and χ_0 ,

$$T^\perp(t) = T(t_0) 2\eta_D(t_0)t_0 \times \begin{cases} \frac{1}{1-3\alpha} \left[\left(\frac{t}{t_0} \right)^{1-3\alpha} - 1 \right] & \alpha < \frac{1}{3} \\ \ln \left(\frac{t}{t_0} \right) & \alpha = \frac{1}{3} \end{cases}. \quad (\text{A29})$$

Similarly, for T_z we have

$$T^z(t) = T(t_0) 2\eta_D(t_0)t_0 \left(\frac{t_0}{t} \right)^2 \frac{1}{3-3\alpha} \left[\left(\frac{t}{t_0} \right)^{3-3\alpha} - 1 \right]. \quad (\text{A30})$$

For small χ the effect of rescattering is to convolute the original transverse momentum distribution with a Gaussian of transverse width $MT^\perp(t)$ and the original longitudinal momentum distribution with a Gaussian of width $MT^z(t)$.

For large values of χ the system approaches equilibrium and memory of the original distribution is lost. The final distribution is a Gaussian which is quite close to the thermal distribution. In this limit the effective temperatures in the transverse and longitudinal directions are

$$T^\perp(t_f) = T(t_f) \left(1 + \frac{\alpha}{2\eta_D(t_f)t_f} \right), \quad (\text{A31})$$

$$T^z(t_f) = T(t_f) \left(1 - \frac{2 - \alpha}{2\eta_D(t_f)t_f} \right). \quad (\text{A32})$$

Thus, the mean squared transverse momentum is slightly *larger* than the equilibrium expectation by an amount of order $1/(2\eta_D(t_f)t_f)$. The longitudinal momentum is slightly *smaller* than the equilibrium value by a similar amount. These corrections are reminiscent of viscous corrections to the stress energy tensor.

APPENDIX B: DETAILS OF LEADING-ORDER CALCULATIONS

In this appendix we provide the complete details of the derivations of the momentum diffusion and energy loss coefficients discussed in the main text.

1. Matrix elements

We begin by proving that the matrix elements given in Eq. (2.9) are correct. The vacuum matrix elements are most easily found in the rest frame of the heavy quark where only t -channel gluon exchange contributes. The external gluon polarization sum is performed with two transverse polarization vectors which are purely spatial in this frame. The amplitude for gluon exchange is $\sim P \cdot K/Q^2$ while the amplitude for a Compton process involves

$$\mathcal{M}_{\text{Compton}} \simeq \bar{u}(p)\not{\epsilon}(-i\not{P} - i\not{K} - M)^{-1}\not{\epsilon}'u(p) \sim \text{Tr}(-i\not{P} + m)\not{\epsilon}\frac{-i\not{P} - i\not{K} + M}{(P + K)^2 + m^2}\not{\epsilon}'. \quad (\text{B1})$$

Since P^μ is purely temporal, ϵ anti-commutes across it, leading to $\mathcal{M}_{\text{Compton}} \sim (P \cdot K)/(P \cdot K)$, which is smaller by a factor of k/M than the gluon exchange amplitude. Therefore, the Compton amplitude can be ignored.

Up to a color factor, the squared matrix elements for the scattering of a heavy fermion with a quark or gluon via t -channel exchange can be written in the following way:

$$|\mathcal{M}|^2 \propto L_{\mu\nu}(P) M_{\alpha\beta}(K, K') G^{\mu\alpha}(Q) G_{\nu\beta}(Q). \quad (\text{B2})$$

Here $G^{\mu\alpha}(Q)$ is the internal gluon propagator which we will take to be in Feynman gauge $\eta^{\mu\alpha}/Q^2$. Tracing over the heavy fermion line, one easily finds

$$L_{\mu\nu}(P) = 4P_\mu P_\nu. \quad (\text{B3})$$

This result is independent of the spin of the heavy particle and depends only on the approximation that its mass is much larger than the Q^2 of the process. For scattering with a light quark, tracing over the light fermion line yields

$$4P_\mu P_\nu M^{\mu\nu} = 16M^2 k^2 (1 + \cos \theta_{kk'}) , \quad (\text{B4})$$

where \mathbf{k} , $\mathbf{k}' = \mathbf{k} - \mathbf{q}$ are the bath particle momenta before and after the collision. For scattering with a gauge boson, contracting the three gluon vertex with the polarization vectors yields

$$4P_\mu P_\nu M^{\mu\nu} = 4 \left[P^\mu ((K_\mu + K'_\mu) \epsilon \cdot \epsilon' - \epsilon_\mu (K - Q) \cdot \epsilon' - \epsilon'_\mu (K' + Q) \cdot \epsilon) \right]^2 . \quad (\text{B5})$$

Using $\epsilon \cdot P = \epsilon' \cdot P = 0$, we have

$$4P_\mu P_\nu M^{\mu\nu} = 16M^2 k^2 (\epsilon \cdot \epsilon')^2 = 16M^2 k^2 (1 + \cos^2 \theta_{kk'}) . \quad (\text{B6})$$

Next we find a covariant expression for the rest-frame angle $\cos \theta_{kk'}$. Since Q is purely spatial and K and K' have the same energy in this frame, we have that $\mathbf{k}' = \mathbf{k} - \mathbf{q}$ and $K'^2 = 0 = K^2 - 2K \cdot Q + Q^2$. Further, $K \cdot K' = k^2 (1 - \cos \theta_{kk'}) = K \cdot (K - Q) = -K \cdot Q = -Q^2/2$. Finally, $k^2 = (K \cdot P)^2 / M^2$. Therefore,

$$\cos \theta_{kk'} = 1 - \frac{Q^2 M^2}{2(K \cdot P)^2} . \quad (\text{B7})$$

Using this, along with $M^2 k^2 = (K \cdot P)^2$, allows us to covariantize the expressions we just found, resulting in Eq. (3.6).

2. Momentum Diffusion – Non-Relativistic Case

Next complete the calculation of Section II. The matrix elements are screened replacing the t -channel gluon propagator in Eq. (B2) with the HTL propagator. This is most easily done in Coulomb gauge, where the HTL propagator in the plasma frame is

$$G_{\mu\nu}(Q) = \frac{-\delta_{\mu 0} \delta_{\nu 0}}{q^2 + \Pi_{00}} + \frac{\delta_{ij} - \hat{q}_i \hat{q}_j}{q^2 - \omega^2 + \Pi_{\text{T}}} . \quad (\text{B8})$$

The substitution $\mu \rightarrow i$ indicates that only the spatial parts participate. Explicit expressions for the HTL self-energies are [59, 60]

$$\Pi_{\text{T}}(\omega, \mathbf{q}) = m_{\text{D}}^2 \left\{ \frac{\omega^2}{2q^2} + \frac{\omega (q^2 - \omega^2)}{4q^3} \left[\ln \left(\frac{q + \omega}{q - \omega} \right) - i\pi \right] \right\} , \quad (\text{B9})$$

$$\Pi_{00}(\omega, \mathbf{q}) = m_{\text{D}}^2 \left\{ 1 - \frac{\omega}{2q} \left[\ln \left(\frac{q + \omega}{q - \omega} \right) - i\pi \right] \right\} . \quad (\text{B10})$$

Since heavy quark is approximately at rest in the rest frame of the plasma $P^\mu = (M, 0)$, only the temporal part of the gauge boson propagator $G^{00}(Q)$ enters when computing the squared matrix elements in Eq. (B2). For the case of momentum diffusion studied here the energy transfer ω is small and the HTL correction reduces to simple Debye screening,

$1/Q^2 = 1/q^2 \rightarrow 1/(q^2 + m_D^2)$. With these observations and the results of the preceding section, the screened matrix elements Eq. (2.9) are reproduced.

The total momentum diffusion constant is then,

$$3\kappa = \frac{1}{2M} \int \frac{d^3\mathbf{k}d^3\mathbf{k}'d^3\mathbf{q}}{(2\pi)^9 8k^0 k'^0 M} (2\pi)^3 \delta^3(\mathbf{k}' - \mathbf{q} - \mathbf{k}) 2\pi \delta(k' - k) \mathbf{q}^2 \times \\ \times [N_f |\mathcal{M}|_{\text{quark}}^2 n_f(k)(1 - n_f(k')) + |\mathcal{M}|_{\text{gluon}}^2 n_b(k)(1 + n_b(k'))] . \quad (\text{B11})$$

We use the 3-momentum delta function to perform the \mathbf{k}' integration and rewrite the the \mathbf{q} integration as

$$\int \frac{d^3\mathbf{q}}{(2\pi)^3} = \frac{1}{4\pi^2} \int q^2 dq \int_{-1}^1 d \cos \theta_{\mathbf{k}\mathbf{q}} . \quad (\text{B12})$$

Using the energy delta function to perform the $\cos \theta_{\mathbf{k}\mathbf{q}}$ integral and noting the relation, $\cos \theta_{\mathbf{k}\mathbf{k}'} = 1 - q^2/(2k^2)$, we have

$$3\kappa = \frac{C_H g^4}{4\pi^3} \int_0^\infty k^2 dk \int_0^{2k} q dq \frac{q^2}{(q^2 + m_D^2)^2} \times \\ \times \left[N_f \frac{e^{k/T}}{(e^{k/T} + 1)^2} \left(2 - \frac{q^2}{2k^2} \right) + N_c \frac{e^{k/T}}{(e^{k/T} - 1)^2} \left(2 - \frac{q^2}{k^2} + \frac{q^4}{4k^4} \right) \right] . \quad (\text{B13})$$

In performing the q integral, we may drop resulting terms which are subleading in m_D/k , because the dominant contribution is from $k \gtrsim T$, where this ratio is small. The q integral in the small m_D/k limit gives

$$3\kappa = \frac{C_H g^4}{4\pi^3} \int_0^\infty k^2 dk \left[\log \frac{4k^2}{m_D^2} - 2 \right] \left[N_f \frac{e^{k/T}}{(e^{k/T} + 1)^2} + N_c \frac{e^{k/T}}{(e^{k/T} - 1)^2} \right] . \quad (\text{B14})$$

The remaining k integral is straightforward and yields

$$3\kappa = \frac{C_H g^4 T^3}{6\pi} \left[N_c \left(\log \frac{2T}{m_D} + \frac{1}{2} - \gamma_E + \frac{\zeta'(2)}{\zeta(2)} \right) + \frac{N_f}{2} \left(\log \frac{4T}{m_D} + \frac{1}{2} - \gamma_E + \frac{\zeta'(2)}{\zeta(2)} \right) \right] . \quad (\text{B15})$$

Finally, the relation between κ and the diffusion coefficient can be used to determine the diffusion coefficient given in the text.

Finally, let us indicate how Eq. (B13) may be used to calculate the diffusion coefficient of a heavy quark in Molnar's parton cascade model. In this model, α_s is related to the total gluon-gluon cross section via, $\sigma_0 = \frac{4\pi C_A^2 \alpha_s^2}{d_A \mu_D^2}$, where $d_A = N_c^2 - 1$ is the dimension of the adjoint representation, and μ_D is a fixed Debye mass. The particles obey classical statistics and therefore $f(1 \pm f)$ is replaced by $Ce^{-p/T}$, where the constant C is adjusted to reproduce the density of the classical particles for each species. With these modifications Eq. (B13) becomes

$$3\kappa = \frac{\sigma_0 \mu_D^2}{2T^3} \int_0^\infty k^2 dk \int_0^{2k} q dq \frac{q^2}{(q^2 + \mu_D^2)^2} \times \\ \times \left[\left(\frac{C_F}{C_A} \right)^2 n_q e^{-k/T} \left(2 - \frac{q^2}{2k^2} \right) + \frac{C_F}{C_A} n_g e^{-k/T} \left(2 - \frac{q^2}{k^2} + \frac{q^4}{4k^4} \right) \right] . \quad (\text{B16})$$

where n_q is the density of quarks plus anti-quarks and n_g is the density of gluons. The total particle density is $n_0 = n_q + n_g$. The form for the diffusion coefficient given in the text Eq. (5.13) follows from Eq. (B16) and the relation between κ and D .

3. Phase Space

In order to calculate the transport coefficients we need to integrate over the phase space in Eq. (3.3). In this sub appendix we will adapt the integration technology of Baym *et al.* [41] to the peculiarities of the heavy quark phase space.

The desired phase space integration domain is

$$\frac{1}{2p^0} \int \frac{d^3\mathbf{k}d^3\mathbf{k}'d^3\mathbf{p}'}{(2\pi)^9 8k^0 k'^0 p'^0} (2\pi)^4 \delta^4(P + K - P' - K'). \quad (\text{B17})$$

We use the spatial delta functions to perform the \mathbf{p}' integration and shift variables to integrate over the momentum transfer $\mathbf{q} \equiv \mathbf{k} - \mathbf{k}'$ rather than \mathbf{k}' . Define the angles $\cos\theta_{kq}$ and $\cos\theta_{pq}$ to be the angles between the \mathbf{k} and \mathbf{q} vectors and the \mathbf{p} and \mathbf{q} vectors, and $\phi_{q;pk}$ to be the angle between the plane containing q, p and the plane containing q, k . Also note that $p'^0 = \sqrt{M^2 + (\mathbf{p} + \mathbf{q})^2}$. Taking \mathbf{p} large, and noting that $v \equiv p/p^0$ is the velocity, this becomes $p'^0 = p^0 + qv \cos\theta_{pq}$ plus terms of order q^2/p^0 which are small. In the denominator, the approximation $p'^0 = p^0$ is good enough.

The phase space becomes,

$$\frac{1}{16(p^0)^2} \frac{1}{(2\pi)^3} \int_0^\infty \frac{kdkq^2dq}{k'} \int_{-1}^1 d\cos\theta_{pq} d\cos\theta_{kq} \int_0^{2\pi} \frac{d\phi_{q;kp}}{2\pi} \delta(p^0 - p'^0 + k - k'). \quad (\text{B18})$$

Now we introduce the integration variable ω

$$1 = \int d\omega \delta(\omega - p'^0 + p^0), \quad (\text{B19})$$

which is the energy transferred to the heavy particle. We now perform the two $\cos\theta$ integrations using kinematic relations to rewrite the delta functions as

$$\begin{aligned} \delta(\omega + p - p') &= \frac{1}{vq} \delta\left(\cos\theta_{pq} - \frac{\omega}{qv}\right), \\ \delta(\omega + k' - k) &= \frac{k'}{kq} \delta\left(\cos\theta_{kq} - \frac{\omega}{q} + \frac{\omega^2 - q^2}{2kq}\right) \Theta(k - \omega). \end{aligned} \quad (\text{B20})$$

The phase space integration becomes

$$\frac{1}{16(p^0)^2} \frac{1}{(2\pi)^3} \int_0^\infty dq \int_{-vq}^{vq} \frac{d\omega}{v} \int_{\frac{\omega+q}{2}}^\infty dk \int_0^{2\pi} \frac{d\phi_{q;kp}}{2\pi}. \quad (\text{B21})$$

When q is small, the lower limit on k can be taken to 0 and $\cos\theta_{kq} \simeq \omega/q$.

4. Energy Loss and Momentum Diffusion – Relativistic Case

Next we will complete the calculation of energy loss and momentum diffusion of Section III B. The procedure is straightforward though somewhat cumbersome. We calculate

the matrix elements with the HTL propagator, substitute the matrix elements into the expressions for the transport coefficients (Eq. (3.3)), and finally integrate over the phase space numerically, as parametrized above.

First we write the matrix elements by inserting the HTL propagator Eq. (B8) into Eq. (B2) and rewrite the resulting expression in terms of the integration variables introduced in the previous sub appendix. Generally, the matrix elements squared are of the form: $|\mathcal{M}|^2 = A + B \cos(\phi_{q:kp}) + C \cos^2(\phi_{q:kp})$. After averaging over this azimuthal angle the matrix element becomes, $\langle \mathcal{M}^2 \rangle_\phi = A + C/2$. For a light quark scattering off a heavy quark, $\langle \mathcal{M}^2 \rangle_\phi$ becomes

$$[\text{cf}] 16(p^0)^2 \left(\frac{4k(k-\omega) - [q^2 - \omega^2]}{2|q^2 + \Pi_L|^2} + \frac{[4k(k-\omega) + (q^2 + \omega^2)][v^2 q^2 - \omega^2][q^2 - \omega^2]}{4q^4 |q^2 - \omega^2 + \Pi_T|^2} \right), \quad (\text{B22})$$

where [cf] denotes the color factor, $[2C_H g^4/2]$ as in Eq. (3.6).

For gluon scattering, essentially the same procedure is followed. However, the result suffers from ambiguities unless the coupling is really small, as discussed in [43]. We will follow the prescription of that work and write the gluon matrix element as the scattering of a fictitious quark (with the color charge of a gluon) plus an infrared finite remainder. To this ephemeral quark we will then apply the HTL corrections and ignore corrections to the finite piece. This procedure is correct to leading order since HTL corrections are only needed for the eikonal vertex, which is independent of the spin of the hard particle. This prescription does something reasonable when m_D/T becomes of order one. Implementing this discussion, we compare the quark and gluon matrix elements in Eq. (3.6) and add

$$[\text{cf}] 16 \left(\frac{(p^0)^2(v^2 - 1)}{2(q^2 - w^2)} + \left\langle \frac{M^4}{4(P \cdot K)^2} \right\rangle_\phi \right), \quad (\text{B23})$$

to the quark expression, Eq. (B22), to obtain the gluon squared matrix element, $\langle M^2 \rangle_\phi$. The color factor [cf] is $[N_c C_H g^4]$ for gluon case. We have not written out the $M^4/4(P \cdot K)^2$ term because it is awkward in this choice of integration variables and will be integrated over separately.

To integrate the $M^4/4(P \cdot K)^2$ term we use a different parametrization of the phase space integrals. We do not introduce q , but align \mathbf{p} with the z axis:

$$\begin{aligned} & \int \frac{d^3 k d^3 k' d^3 p'}{(2\pi)^9 16(p^0)^2 k^0 k'^0} (2\pi)^4 \delta^4(p + k - p' - k') \\ &= \frac{1}{16(p^0)^2} \frac{1}{(2\pi)^3} \int_0^1 k dk k' dk' \int_{-1}^1 d \cos \theta_{kp} d \cos \theta_{k'p} \int_0^{2\pi} \frac{d\phi_{p;kk'}}{2\pi} \delta(k - k' + p^0 - p'^0). \end{aligned} \quad (\text{B24})$$

In these variables $p'^0 = p^0 + vk \cos \theta_{kp} - vk' \cos \theta_{k'p}$. Next we introduce a new integration variable

$$1 = \int_0^\infty d\omega \delta(\omega - k(1 - v \cos \theta_{kp})), \quad (\text{B25})$$

and use the two delta functions to perform the two angular integrations, which yields

$$\frac{1}{16(p^0)^2} \frac{1}{(2\pi)^3} \int_0^\infty d\omega \int_{\frac{\omega}{1+v}}^{\frac{\omega}{1-v}} \frac{dk dk'}{v v} \int_0^{2\pi} \frac{d\phi_{p;kk'}}{2\pi}. \quad (\text{B26})$$

The energy transfer is $q^0 = k' - k$ and $P \cdot K = p^0 k(-1 + v \cos \theta_{pk}) = -\omega p^0$. The vector \mathbf{q} is complicated in this coordinate system, but this vector is not needed to integrate $M^4/4(P \cdot K)^2$. With this parametrization, the $\phi_{p;kk'}$ integral over $M^4/4(P \cdot K)^2$ can immediately be performed, leaving three integrals that are performed numerically.

In summary, we take the screened matrix elements insert them into the expressions for the transport coefficients and finally perform the phase space integrals. The results of this procedure is illustrated in Fig. 2 and has been discussed in the main text.

Analytic expressions for the transport coefficients can be derived to leading logarithm in T/m_D [38]. We will discuss the energy loss coefficient and leave the details of the other transport coefficients to the reader. For $q \ll T$ the matrix elements for the scattering of a light quark or gluon on a heavy quark are identical up to a color factor

$$\langle \mathcal{M}^2 \rangle_\phi = [\text{cf}] 16 \left(2 \frac{(p^0 k)^2}{|q^2 + \Pi_{00}|^2} + \frac{(p^0 k)^2 (q^2 - \omega^2)(q^2 v^2 - \omega^2)}{|q^2 - \omega^2 + \Pi_T|^2} \right). \quad (\text{B27})$$

Again the color factor [cf] is $[2C_H g^4/2]$ for quarks and $[N_c C_H g^4]$ for gluons. For small q and ω the weight factor in Eq. (3.3) is

$$\frac{\omega}{2v} (n[k-\omega](1 \pm n[k]) - n[k](1 \pm n[k-\omega])) \simeq \frac{\omega^2}{2vT} n[k](1 \pm n[k]). \quad (\text{B28})$$

Next we insert this weight factor and the small q matrix elements into Eq. (3.3) and Eq. (B21) for the energy loss rate. After performing the integral over k , the momentum loss rate is

$$\frac{dp}{dt} = v \left(N_c + \frac{N_f}{2} \right) \frac{C_H g^4 T^2}{12\pi} \int dq \int_{-vq}^{vq} \frac{d\omega}{v} \frac{\omega^2}{2v^2} \left(\frac{q^4}{|q^2 + \Pi_{00}|^2} + \frac{(q^2 - \omega^2)(v^2 q^2 - \omega^2)}{2|q^2 - \omega^2 + \Pi_T|^2} \right). \quad (\text{B29})$$

To determine the leading-log coefficient, one should find the coefficient of dq/q when one drops the self-energies in this expression. Following this prescription and performing the ω integral, we transform Eq. (B29) into

$$\frac{dp}{dt} \simeq v \left(N_c + \frac{N_f}{2} \right) \frac{C_H g^4 T^2}{24\pi} \left(\frac{1}{v^2} - \frac{1-v^2}{2v^3} \log \frac{1+v}{1-v} \right) \log(T/m_D). \quad (\text{B30})$$

The coefficient in front of $\log(T/m_D)$ is referred to as the leading-log coefficient below. A similar analysis but with different weight functions gives the leading log expressions for the transverse and longitudinal momentum diffusion coefficients given in the text, Eq. (3.9).

A procedure which is correct to next-to-leading logarithm was formulated by Braaten and Yuan [61] and then used for heavy quark energy loss by Braaten and Thoma [38]. Here the momentum integration is divided up into a soft region $q < q^*$ and a hard region $q^* < q$, where q^* is some intermediate scale $m_D \ll q^* \ll T$. To determine the soft contribution to transport coefficient, one should integrate Eq. (B29) up to q^* with the self energies. For $q^* \gg m_D$, this integral is a number $A_{\text{soft}}(v)$ plus the leading-log coefficient times $\log(q^*/m_D)$. To determine the hard contribution to the transport coefficient, one should drop the self-energies in Eq. (B22) and numerically integrate the matrix elements over the phase space with $q > q^*$. For $T \gg q^*$, this integral is a number $A_{\text{hard}}(v)$, plus the leading-log coefficient times $\log(T/q^*)$. The sum of the hard and soft contributions is independent of q^* and determines

v	$A_b(v)$	$A_f(v)$	$B_b(v)$	$B_f(v)$	$C_b(v)$	$C_f(v)$
0.05	0.0488	0.7420	0.0503	0.7440	0.0502	0.7437
0.10	0.0567	0.7499	0.0617	0.7570	0.0620	0.7568
0.15	0.0692	0.7624	0.0793	0.7774	0.0813	0.7782
0.20	0.0861	0.7793	0.1026	0.8047	0.1081	0.8080
0.25	0.1074	0.8006	0.1312	0.8383	0.1425	0.8464
0.30	0.1331	0.8262	0.1648	0.8782	0.1851	0.8941
0.35	0.1633	0.8564	0.2032	0.9240	0.2366	0.9519
0.40	0.1981	0.8913	0.2462	0.9758	0.2981	1.0211
0.45	0.2380	0.9312	0.2937	1.0334	0.3712	1.1036
0.50	0.2834	0.9765	0.3459	1.0973	0.4580	1.2018
0.55	0.3348	1.0280	0.4029	1.1677	0.5617	1.3195
0.60	0.3933	1.0864	0.4653	1.2456	0.6871	1.4622
0.65	0.4600	1.1532	0.5339	1.3321	0.8415	1.6383
0.70	0.5371	1.2303	0.6101	1.4293	1.0369	1.8616
0.75	0.6276	1.3208	0.6963	1.5408	1.2943	2.1566
0.80	0.7368	1.4299	0.7969	1.6728	1.6549	2.5703
0.85	0.8747	1.5678	0.9200	1.8374	2.2119	3.2097
0.90	1.0641	1.7572	1.0848	2.0625	3.2366	4.3846
0.95	1.3796	2.0728	1.3528	2.4390	6.0376	7.5840

TABLE I: The six functions of velocity $A(v)$, $B(v)$, and $C(v)$ for bosons (b) and fermions (f) are defined by Eqs. (B31–B33) and parametrize the transport properties of a heavy particle in the QGP.

the transport coefficient. The results of this procedure is the following parametrization of the transport properties of a heavy quark in the QGP

$$\frac{dp}{dt} = \frac{C_H g^4 T^2}{24\pi} v \left(\frac{1}{v^2} - \frac{1-v^2}{2v^3} \log \frac{1+v}{1-v} \right) \times \left[N_c (\log(T/m_D) + A_b(v)) + \frac{N_f}{2} (\log(T/m_D) + A_f(v)) \right], \quad (\text{B31})$$

$$\kappa_T = \frac{C_H g^4 T^3}{12\pi} \left(\frac{3}{2} - \frac{1}{2v^2} + \frac{(1-v^2)^2}{4v^3} \log \frac{1+v}{1-v} \right) \times \left[N_c (\log(T/m_D) + B_b(v)) + \frac{N_f}{2} (\log(T/m_D) + B_f(v)) \right], \quad (\text{B32})$$

$$\kappa_L = \frac{C_H g^4 T^3}{12\pi} \left(\frac{1}{v^2} - \frac{1-v^2}{2v^3} \log \frac{1+v}{1-v} \right) \times \left[N_c (\log(T/m_D) + C_b(v)) + \frac{N_f}{2} (\log(T/m_D) + C_f(v)) \right]. \quad (\text{B33})$$

The coefficients $A(v)$, $B(v)$ and $C(v)$ for bosons and fermions are tabulated as a function of velocity in Table I.

-
- [1] see Quark Matter 2004, J. Phys. G **30**, for recent developments.
- [2] J. Adams *et al.* [STAR Collaboration], arXiv:nucl-ex/0409033.
- [3] C. Adler *et al.* [STAR Collaboration], Phys. Rev. C **66**, 034904 (2002) [arXiv:nucl-ex/0206001].
- [4] K. Adcox *et al.* [PHENIX Collaboration], Phys. Rev. Lett. **89**, 212301 (2002) [arXiv:nucl-ex/0204005].
- [5] C. M. Vale [the PHOBOS Collaboration], arXiv:nucl-ex/0410008.
- [6] B. B. Back *et al.* [PHOBOS Collaboration], Phys. Rev. Lett. **89**, 222301 (2002) [arXiv:nucl-ex/0205021].
- [7] D. Molnar and M. Gyulassy, Nucl. Phys. A **697**, 495 (2002) [Erratum-ibid. A **703**, 893 (2002)] [arXiv:nucl-th/0104073].
- [8] T. Hirano, J. Phys. G **30**, S845 (2004) [arXiv:nucl-th/0403042].
- [9] D. Teaney, J. Lauret and E. V. Shuryak, arXiv:nucl-th/0110037. *ibid*, Phys. Rev. Lett. **86**, 4783 (2001) [arXiv:nucl-th/0011058].
- [10] P. F. Kolb, P. Huovinen, U. W. Heinz and H. Heiselberg, Phys. Lett. B **500**, 232 (2001) [arXiv:hep-ph/0012137].
- [11] P. Huovinen, P. F. Kolb, U. W. Heinz, P. V. Ruuskanen and S. A. Voloshin, Phys. Lett. B **503**, 58 (2001) [arXiv:hep-ph/0101136].
- [12] D. Molnar and P. Huovinen, arXiv:nucl-th/0404065.
- [13] D. Teaney, Phys. Rev. C **68**, 034913 (2003).
- [14] P. Arnold, J. Lenaghan, G. D. Moore and L. G. Yaffe, arXiv:nucl-th/0409068.
- [15] D. Molnar and S. A. Voloshin, Phys. Rev. Lett. **91**, 092301 (2003) [arXiv:nucl-th/0302014].
- [16] Z. w. Lin and C. M. Ko, Phys. Rev. C **65**, 034904 (2002) [arXiv:nucl-th/0108039].
- [17] R. J. Fries, B. Muller, C. Nonaka and S. A. Bass, Phys. Rev. Lett. **90**, 202303 (2003) [arXiv:nucl-th/0301087].
- [18] V. Greco, C. M. Ko and P. Levai, Phys. Rev. Lett. **90**, 202302 (2003) [arXiv:nucl-th/0301093].
- [19] V. Greco, C. M. Ko and R. Rapp, Phys. Lett. B **595**, 202 (2004) [arXiv:nucl-th/0312100].
- [20] Z. w. Lin and D. Molnar, Phys. Rev. C **68**, 044901 (2003) [arXiv:nucl-th/0304045].
- [21] P. Kovtun, D. T. Son and A. O. Starinets, arXiv:hep-th/0405231.
- [22] S. Batsouli, S. Kelly, M. Gyulassy and J. L. Nagle, Phys. Lett. B **557**, 26 (2003) [arXiv:nucl-th/0212068].
- [23] J. Adams *et al.* [STAR Collaboration], arXiv:nucl-ex/0407006.
- [24] R. Auerbeck [PHENIX Collaboration], arXiv:nucl-ex/0410007.
- [25] S. S. Adler [the PHENIX Collaboration], arXiv:nucl-ex/0409028.
- [26] S. Kelly [PHENIX Collaboration], J. Phys. G **30**, S1189 (2004) [arXiv:nucl-ex/0403057].
- [27] K. Adcox *et al.* [PHENIX Collaboration], Phys. Rev. Lett. **88**, 192303 (2002) [arXiv:nucl-ex/0202002].
- [28] M. Djordjevic and M. Gyulassy, Phys. Lett. B **560**, 37 (2003) [arXiv:nucl-th/0302069].
- [29] M. Djordjevic and M. Gyulassy, Nucl. Phys. A **733**, 265 (2004) [arXiv:nucl-th/0310076].
- [30] Y. L. Dokshitzer and D. E. Kharzeev, Phys. Lett. B **519**, 199 (2001) [arXiv:hep-ph/0106202].
- [31] N. Armesto, C. A. Salgado and U. A. Wiedemann, Phys. Rev. D **69**, 114003 (2004) [arXiv:hep-ph/0312106].
- [32] K. Hagiwara *et al.* [Particle Data Group Collaboration], Phys. Rev. D **66**, 010001 (2002).

- [33] M. G. Mustafa, D. Pal, D. K. Srivastava and M. Thoma, Phys. Lett. B **428**, 234 (1998) [arXiv:nucl-th/9711059].
- [34] M. G. Mustafa, D. Pal and D. K. Srivastava, Phys. Rev. C **57**, 889 (1998) [arXiv:nucl-th/9706001].
- [35] R. Baier, Y. L. Dokshitzer, A. H. Mueller and D. Schiff, JHEP **0109**, 033 (2001) [arXiv:hep-ph/0106347].
- [36] S. Jeon and G. D. Moore, arXiv:hep-ph/0309332.
- [37] M. G. Mustafa and M. H. Thoma, arXiv:hep-ph/0311168.
- [38] E. Braaten and M. H. Thoma, Phys. Rev. D **44**, 2625 (1991). Phys. Rev. D **44**, 1298 (1991).
- [39] P. Romatschke and M. Strickland, arXiv:hep-ph/0408275.
- [40] B. Svetitsky, Phys. Rev. D **37**, 2484 (1988).
- [41] G. Baym, H. Monien, C. J. Pethick and D. G. Ravenhall, Phys. Rev. Lett. **64** (1990) 1867.
- [42] P. Arnold, G. D. Moore and L. G. Yaffe, JHEP **0011**, 001 (2000) [arXiv:hep-ph/0010177].
- [43] P. Arnold, G. D. Moore and L. G. Yaffe, JHEP **0305**, 051 (2003) [arXiv:hep-ph/0302165].
- [44] H. van Hees and R. Rapp, arXiv:nucl-th/0412015.
- [45] M. G. Mustafa, arXiv:hep-ph/0412402.
- [46] D. Molnar, arXiv:nucl-th/0410041.
- [47] B. Zhang, L. W. Chen and C. M. Ko, arXiv:nucl-th/0502056.
- [48] F. Reif, “Fundamentals of Statistical Physics”, Sect. 15.12, McGraw-Hill (1965).
- [49] P. Arnold, Phys. Rev. E **61**, 6091 (2000) [arXiv:hep-ph/9912208]. Phys. Rev. E **61**, 6099 (2000) [arXiv:hep-ph/9912209].
- [50] J. D. Bjorken, Phys. Rev. D **27**, 140 (1983).
- [51] G. Baym, Phys. Lett. B **138** (1984) 18.
- [52] A. E. Pukhov *et al*, [arXiv:hep-ph/9908288].
- [53] T. Sjöstrand *et al*, Comp. Phys. Commun. **135**, 238 (2001) [arXiv:hep-ph/0010017].
- [54] D. J. Higham, SIAM Rev. **43**, 525 (2001).
- [55] N. Borghini, P. M. Dinh and J. Y. Ollitrault, Phys. Rev. C **63**, 054906 (2001) [arXiv:nucl-th/0007063].
- [56] R. S. Bhalerao, N. Borghini and J. Y. Ollitrault, Phys. Lett. B **580**, 157 (2004) [arXiv:nucl-th/0307018].
- [57] D. Molnar, arXiv:nucl-th/0406066.
- [58] D. Molnar, arXiv:nucl-th/0408044.
- [59] O. K. Kalashnikov and V. V. Klimov, Sov. J. Nucl. Phys. **31**, 699 (1980) [Yad. Fiz. **31**, 1357 (1980)].
- [60] H. A. Weldon, Phys. Rev. **D26**, 1394 (1982).
- [61] E. Braaten and T. C. Yuan, Phys. Rev. Lett. **66**, 2183 (1991).